FORELAND STRUCTURE AND KARSTIC GROUND WATER CIRCULATION IN THE EASTERN GROS VENTRE RANGE, WYOMING

John P. Mills
Peter Huntoon

May 1989 WWRC-89-02

Department of Geology and Geophysics
University of Wyoming
Laramie, Wyoming

Research Project Technical Completion Report
(USGS G-1600, Project No. 02)

Prepared for:
U.S. Department of the Interior
Geological Survey

The activities on which this report is based were financed in part by the Department of the Interior, U.S. Geological Survey, through the Wyoming Water Research Center.

Wyoming Water Research Center
University of Wyoming
Laramie, Wyoming

ACKNOWLEDGMENTS

The author wishes to express sincere appreciation to Dr. P. W. Huntoon for assistance in preparing the manuscript and for acquiring funding for this project from the Wyoming Water Research Center. Comments and suggestions offered by Dr. J. D. Love, Dr. D. L. Blackstone, and Dr. R. Marston enhanced the material presented in the text. Dr. D. R. Lageson piloted the airplane used for aerial photography and provided helpful comments and suggestions. The American Wilderness Leadership School provided support, encouragement, and room and board in the field area. I thank all these individuals for their assistance.

TABLE OF CONTENTS

TABLE OF CONTENTS (cont.)

LIST OF FIGURES

LIST OF FIGURES (cont.)

LIST OF FIGURE (cont.)

LIST OF FIGURES (cont.)

LIST OF FIGURES (cont.)

LIST OF APPENDICES

CHAPTER I

INTRODUCTION

Purpose

The objective of this study is to characterize groundwater recharge and storage in the Paleozoic rocks in the eastern Gros Ventre Range, a Laramide foreland uplift in northwest Wyoming. The ground water recharge and storage characteristics of the eastern Gros Ventre Range are a direct result of the foreland style of deformation and the lithologies and permeabilities of the Paleozoic rocks involved in this deformation. Therefore, before discussing ground water recharge and storage in detail, it is necessary to set forth the structural geometry and the lithologic and permeability characteristics of the Paleozoic rocks in the eastern Gros Ventre Range.

Location and Physiographic Setting

The project area outlined in Figure 1 encompasses 270 square miles and is centered on the unforested exposures of erosionally resistant Paleozoic rocks along the crest of the eastern Gros Ventre Range. The crest of the range is at an elevation of 10000 to 11500 feet and stands 3000 to 4000 feet above the surrounding basins.

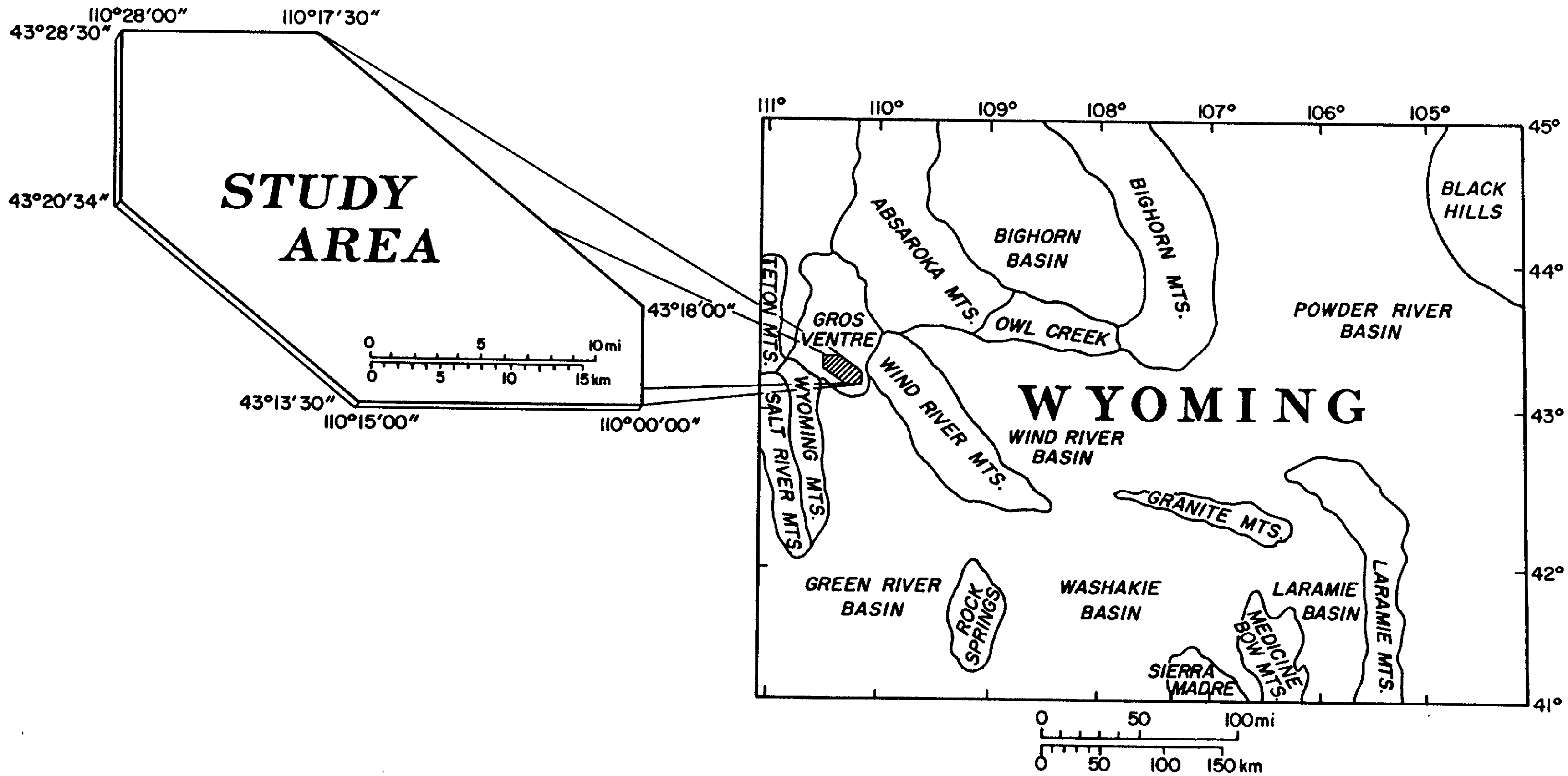

Figure 1. Location of the area in northwest Wyoming treated in this thesis.

Precipitation averages 60 inches per year along the crest of the range, decreasing to less than 20 inches along the flanks (Martner, 1986). Much of the yearly precipitation in the project area is stored in the thick winter snowpack. The late May and June snow melt provides the largest part of the yearly recharge to ground water systems in the eastern Gros Ventre Range.

Geologic and Tectonic Setting

The Gros Ventre Range is a southwest verging faulted anticline lying northwest of and en echelon to the Wind River Range as shown on Figure 2. The anticline plunges southeast into the upper Green River Basin. Figure 3 is a schematic north-south cross section through the anticline showing an asymmetrically folded and thrust-severed forelimb and a mildly deformed homoclinal backlimb.

As shown on Figure 4, approximately 17000 feet of Paleozoic and Mesozoic sedimentary rocks are exposed within the study area. These sedimentary rocks are underlain by Precambrian crystalline igneous and metamorphic rocks. The surrounding Hoback, Green River, and Jackson Hole basins are filled with thousands of feet of Tertiary rocks and are mantled by younger unconsolidated sediments.

Methodology

Figure 5 is a geologic map of the area outlined in

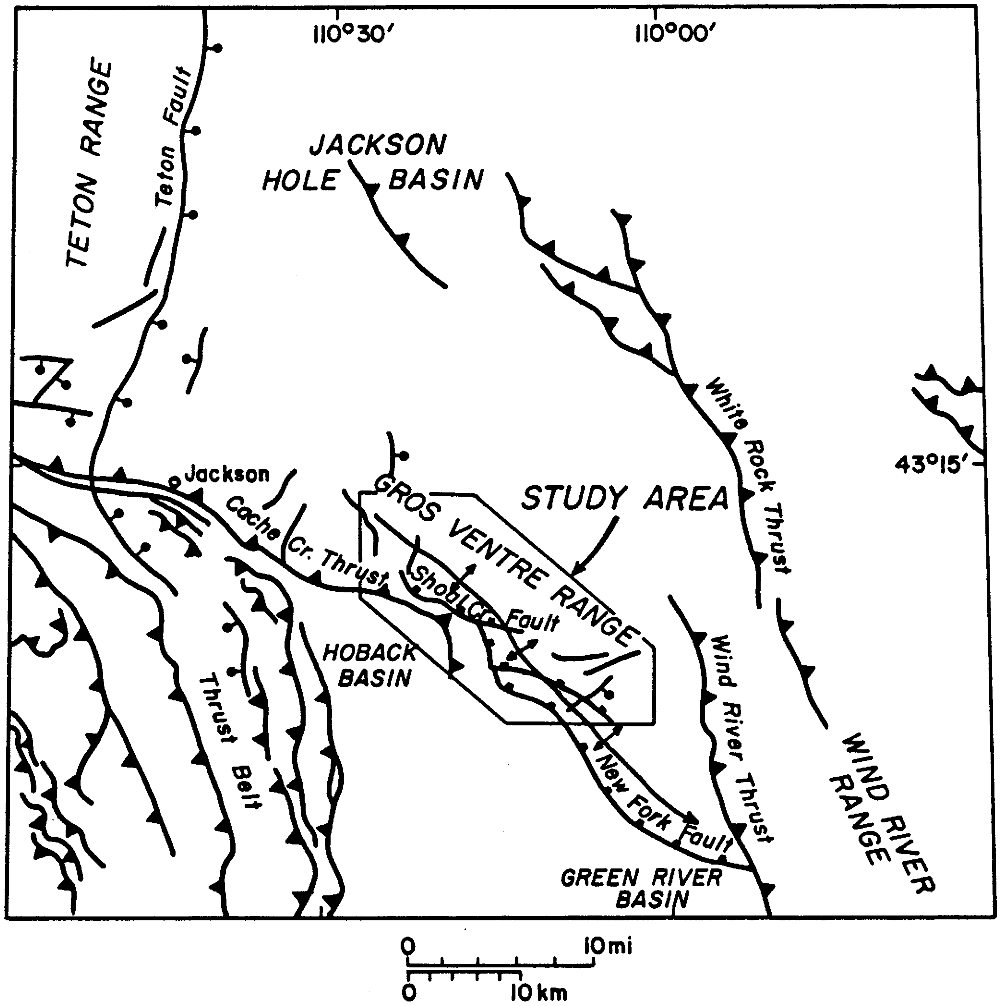

Figure 2. Principal tectonic structures in the region surrounding the project area, northwestern Wyoming.

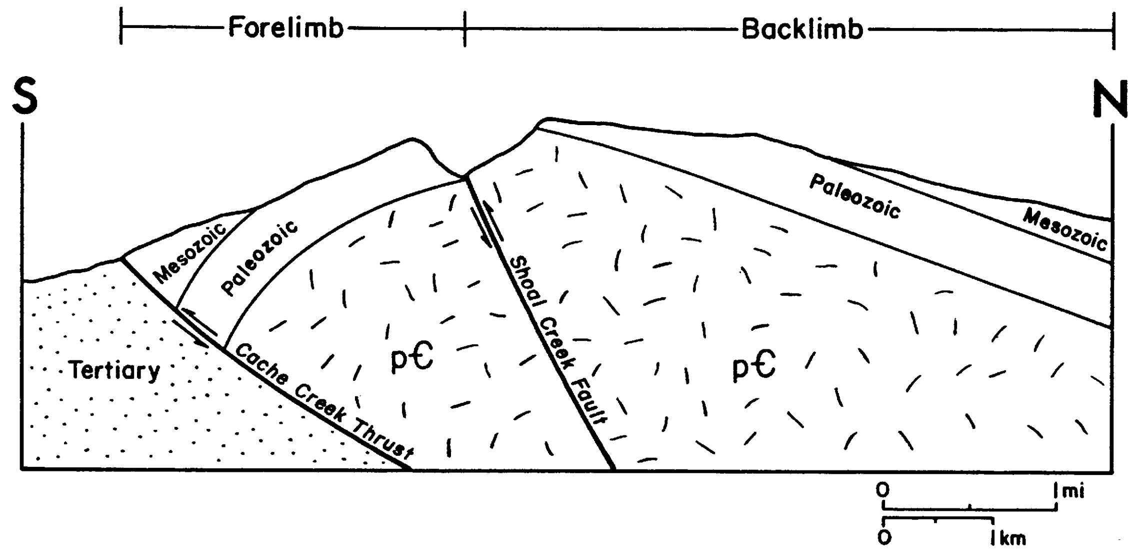

Figure 3. Schematic north-south cross section through the eastern Gros Ventre Range, Wyoming.

Figure 1 and was prepared through field reconnaissance and examination of aerial photography. Published geologic maps by Nelson and Church (1943), Keefer (1964), Dorr and others (1977), Cutler (1984), and Simons and others (1988) were also consulted in the preparation of Figure 5.

The hydrologic data on Figure 6 was compiled during the course of this study and includes the location of springs yielding potentiometric and water chemistry data, boundaries of ground water systems, ground water flow directions, dye trace paths, and the surface traces of faults important to ground water flow. Discharge data for the springs on Figure 6 are listed in Appendix B. Spring discharge was measured by width-depth-velocity gaging techniques. Three dye tracings were conducted with Na-fluorescein. Dye detection was accomplished with activated charcoal (Aley, personal communication).

Fifty-three water samples were collected from springs in order to characterize water qualities in the Paleozoic rocks. The major ion analyses of these samples, listed in Appendix C, where performed at the University of Wyoming rock-water chemistry laboratory.

CHAPTER II

STRUCTURAL GEOLOGY OF THE EASTERN GROS VENTRE RANGE

The structural framework of Paleozoic rocks through which ground water circulates in the eastern Gros Ventre Range is a result of deformation during the Late Cretaceous through early Eocene Laramide orogeny. Laramide foreland ranges like the Gros Ventre Range owe their origin to large scale anticlinal folding and thrusting of the Precambrian and overlying Phanerozoic rocks which comprised the Wyoming foreland basin. The purpose this chapter is to describe the structural geometry of the eastern Gros Ventre Range so that in later chapters ground water circulation through the Paleozoic rocks can be related to this structural geometry.

This study reinterprets some fault geometries shown by Keefer (1964); Cutler, (1984); and Simons and others (1988) in the eastern Gros Ventre Range. Furthermore, the timing relations between movement along the principal faults is revised. These findings are included in this report because they are pertinent to ground water circulation as well as to the regional structural relations of the Gros Ventre Range.

Starting in Late Cretaceous time, the Teton and Gros Ventre ranges rose as a single broad northwest trending foreland arch known as the ancestral Teton-Gros Ventre uplift (Love, 1973, 1977). See Figure 7. The earliest indication of the ancestral Teton-Gros Ventre uplift is the lack of quartzite clasts from the Late Cretaceous Harebell Formation and the Paleocene Pinyon Conglomerate in the Paleocene Hoback Formation of the Hoback Basin. These conglomerates are present in immense quantities in the nearby Jackson Hole Basin but were prevented from moving southward by the ancestral Teton-Gros Ventre uplift (Love, 1973).

The Late Cretaceous and early Paleocene rise of the ancestral Teton-Gros Ventre uplift was accomplished by broad anticlinal warping of the Precambrian and overlying Phanerozoic rocks. Later, during late Paleocene and early Eocene time, the Gros Ventre Range was further uplifted by displacement along large scale thrust and reverse faults along its south flank. Displacement along these faults is as great as 25000 feet.

The eastern Gros Ventre Range was uplifted and thrust west-southwest by displacement along three northeast dipping thrust and reverse faults during late Paleocene and early Eocene time (Wiltschko and Dorr, 1983). As shown on Figure 8, uplift of the eastern range involved successive displacement along the Cache Creek blind thrust, the Cache Creek thrust, and the Shoal Creek-New Fork fault system.

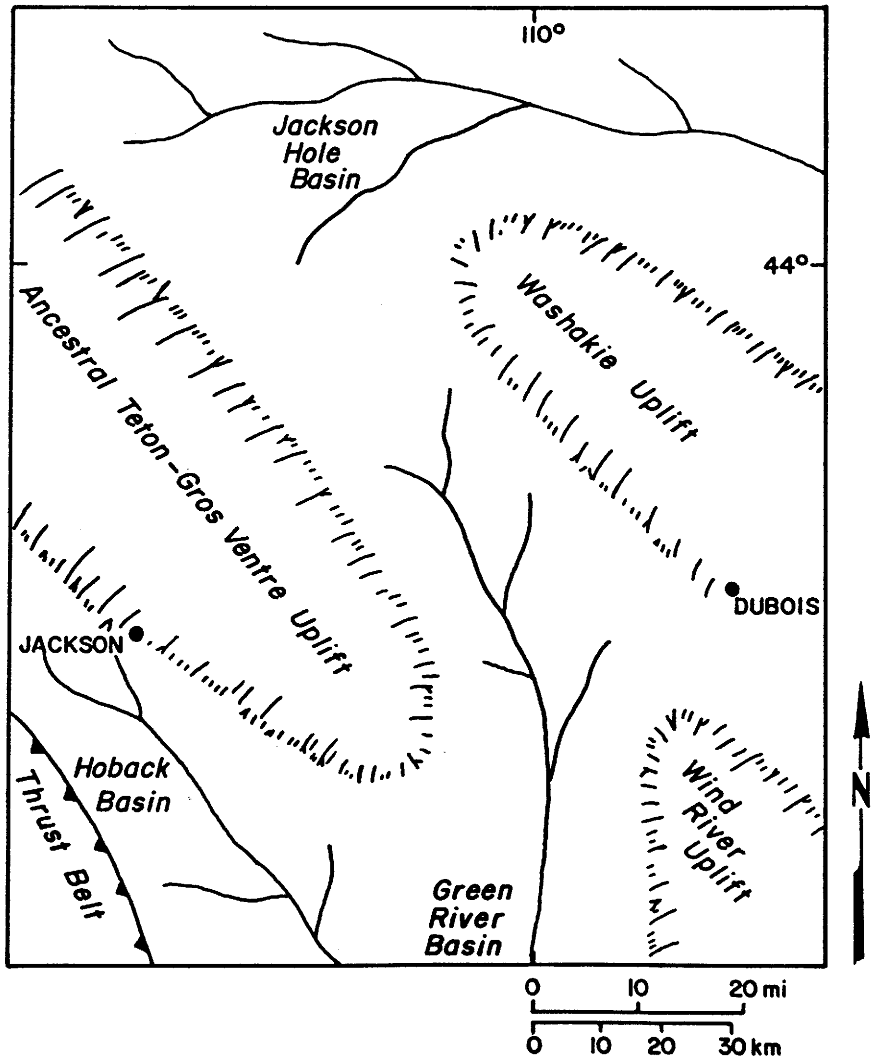

Figure 7. Map showing the reconstructed position of the Late Cretaceous and early Paleocene ancestral Teton-Gros Ventre uplift, northwestern Wyoming. Modified from Love (1973).

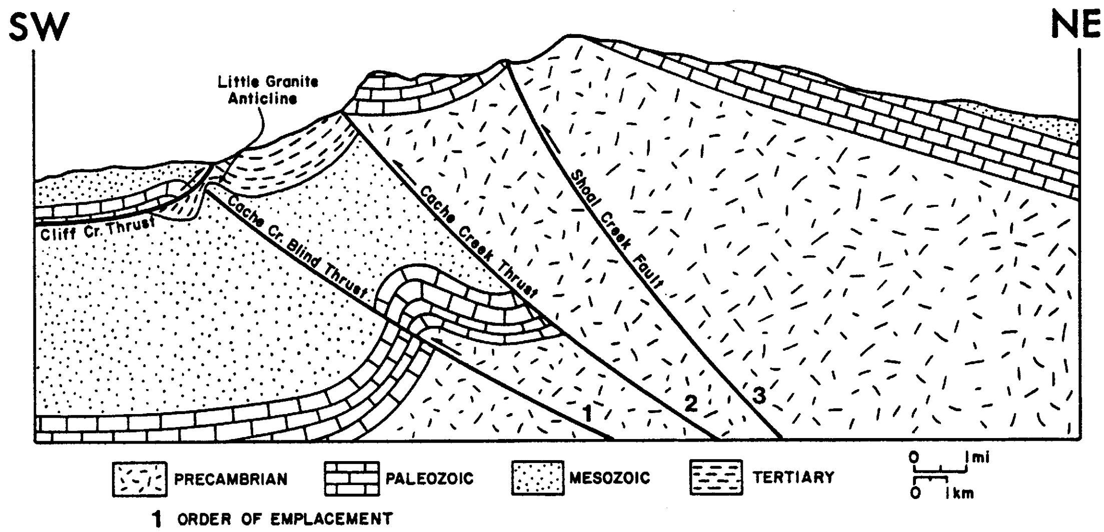

Figure 8. Schematic northeast-southwest cross section showing the position and order of emplacement of the Cache Creek blind thrust, Cache Creek thrust, and Shoal Creek fault in the Gros Ventre Range, Wyoming.

The Cache Creek Blind Thrust

The earliest fault displacement during uplift of the eastern Gros Ventre Range occurred along the Cache Creek blind thrust. See Figure 8. The Cache Creek blind thrust does not reach the surface but is revealed by seismic data in the Hoback Basin where it cores Little Granite anticline shown in Figure 8.

Movement along the Cache Creek blind thrust is dated as late Paleocene by the following rationale. Hunter (1987) shows that late Paleocene Hoback strata folded in the Little Granite anticline was overridden by the Cliff Creek thrust as shown on Figure 8. Dorr and others (1977) report that the Cliff Creek thrust is buried by the early Eocene Lookout Mountain Conglomerate Member of the Wasatch Formation 15 miles to the south. This reveals that movement along the Cliff Creek thrust occurred during latest Paleocene time. Movement along the Cache Creek blind thrust must have occurred after deposition of the late Paleocene Hoback strata folded in Little Granite anticline and prior to latest Paleocene movement along the Cliff Creek thrust (Wiltschko and Dorr, 1983; Hunter, 1987).

The Cache Creek Thrust

By far the most important stage in the development of the eastern Gros Ventre Range was displacement along the Cache Creek thrust. See Figures 5 and 8. Displacement along the Cache Creek thrust produced most of the 25000 feet of structural relief between Precambrian rocks in the Gros Ventre range and those in the adjacent Hoback Basin as shown by Blackstone (1988).

Simons and others (1988) concluded from gravity data that the Cache Creek thrust dips 30 to 45 degrees northeast beneath the Gros Ventre Range. At this dip, at least 25000 feet of northeast-southwest shortening across the Gros Ventre Range is required to produce 25000 feet of structural relief. Preliminary data developed by Lageson (1987) from slickenside lineations along the Cache Creek thrust indicates a strong component of west directed oblique slip. If displacement on the Cache Creek thrust was predominantly west directed reverse oblique slip, then east-west shortening across the Gros Ventre Range is greater than the 25000 feet of northeast-southwest shortening.

Movement along the Cache Creek thrust occurred during late Paleocene and early Eocene time as revealed by: (1) the Cache Creek thrust severs the late Paleocene-early Eocene Skyline Trail Conglomerate Member of the Hoback Formation at Granite Creek as shown in Figure 9, and (2) Paleocene Hoback strata deformed by movement along the Cache Creek thrust is unconformably overlain by undeformed middle early Eocene Pass Peak Formation (Steidtmann, 1971). See Figure 10.

Initial uplift along the Cache Creek thrust was contemporaneous with and responsible for deposition of the

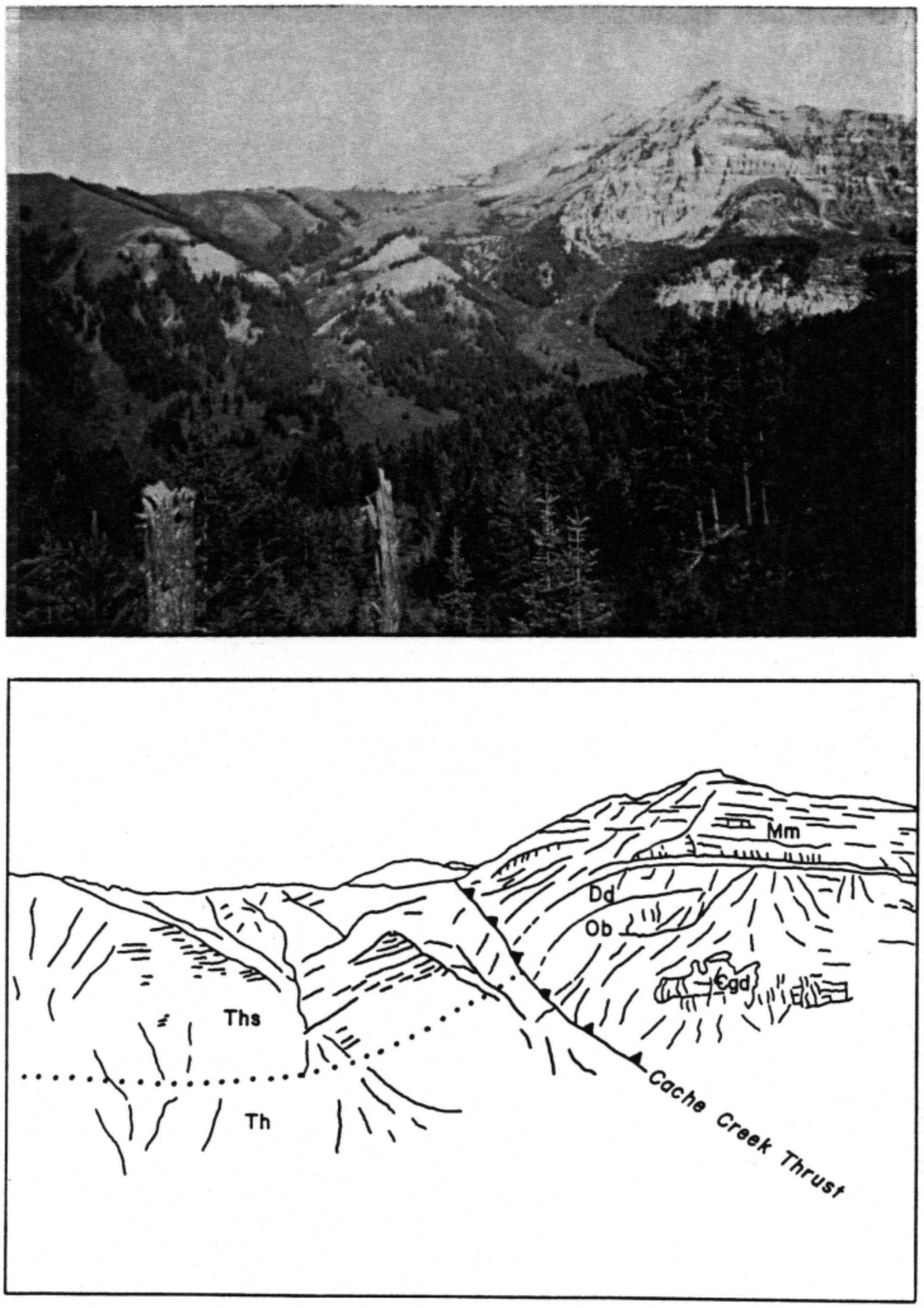

Figure 9. Photograph and line drawing showing the Cache Creek thrust severing the Skyline Trail Conglomerate Member of the Paleocene Hoback Formation near Granite Creek, Gros Ventre Range, Wyoming. View is toward the west. See Figure 5 for stratigraphic unit abbreviations.

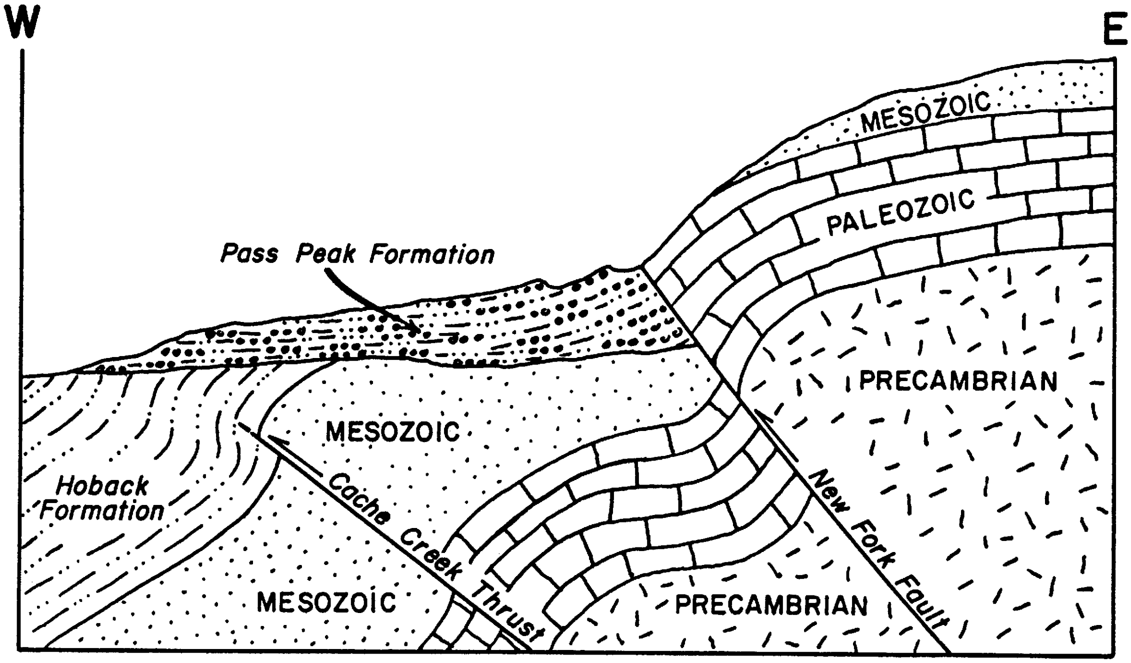

Figure 10. Schematic northeast-southwest cross section through the eastern Gros Ventre Range, Wyoming. Cross section shows undeformed middle early Eocene Pass Peak Formation unconformably overlying deformed Paleocene Hoback Formation and severed by movement along the New Fork fault.

Skyline Trail conglomerate. Therefore, early movement started during late Paleocene time and was probably contemporaneous with late movement on the Cache Creek blind thrust. However, unlike the Cache Creek blind thrust, movement along the Cache Creek thrust continued in early Eocene time and overrode the Skyline Trail conglomerate. Movement ceased prior to deposition of the middle early Eocene Pass Peak Formation.

The Shoal Creek-New Fork Fault System

The last stage in the Laramide compression of the eastern Gros Ventre Range involved displacement along the Shoal Creek-New Fork reverse fault system. The Shoal Creek and New Fork faults transported basement cored blocks westward within the hanging wall of the Cache Creek thrust after movement along the thrust ceased.

Nelson and Church (1943), Keefer (1964), and Simons and others (1988) mapped the Shoal Creek fault as a normal fault. However, as shown on Figures 5 and 11 A-A', west directed reverse dip slip along the north trending segment of the Shoal Creek fault is accommodated northward by east-west fold shortening within the Granite Creek and Crystal Creek anticlines. The 80 degree average rake of slickenside lineations on fractures observed by Lageson (1987) along this segment of the fault confirms west directed reverse dip slip. See Figure 12. Figure 12 also shows the rake of

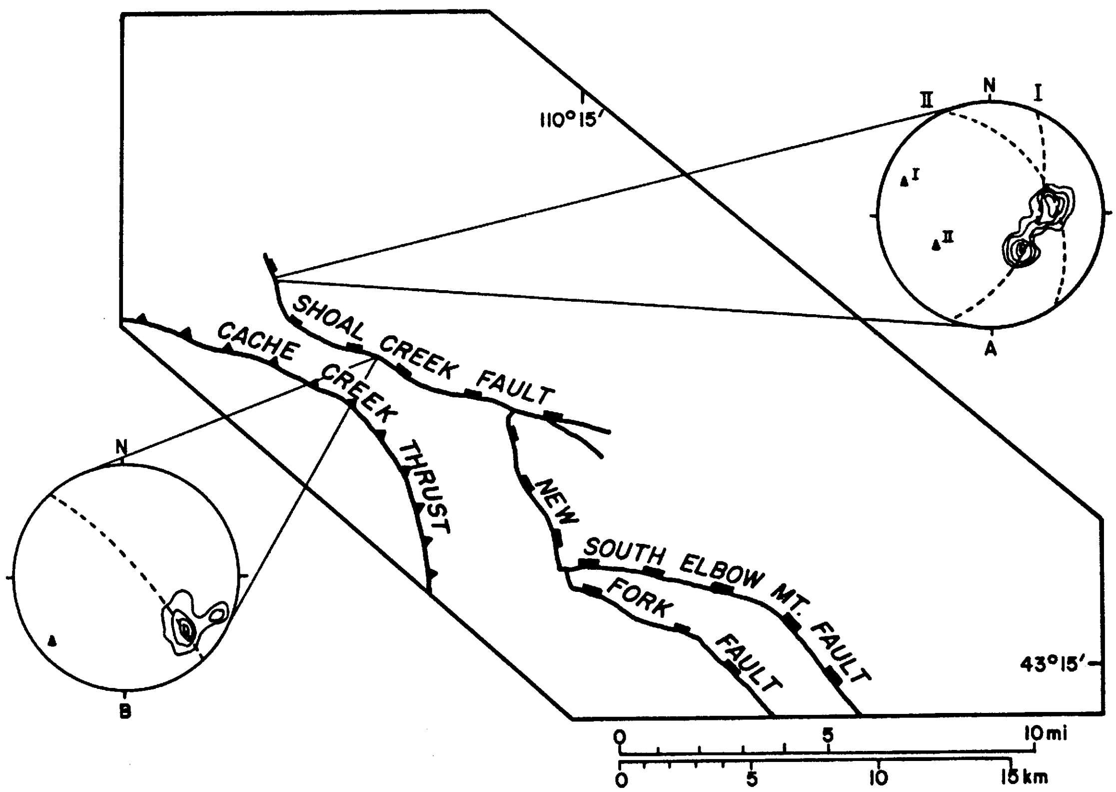

Figure 12. Lower hemisphere equal area projections showing the rake of slickenside lineations on fractures along the Shoal Creek fault in the eastern Gros Ventre Range, Wyoming. Projection A is for fractures along the north trending segment of the Shoal Creek fault. Triangles (I and II) are the average pole positions of fault zone fractures, corresponding to great circles (I and II). Contours show trend and plunge of slickenside lineations (rake). Average rake of lineations indicates predominantly dip slip motion. Projection B is for the east trending segment of the Shoal Creek fault. Triangle is average pole of fault zone fractures. Rake of slickenside lineations indicates strong component of west oblique slip. Modified from Lageson (1987).

slickenside lineations on fractures along the east trending segment of the Shoal Creek fault. The 25 to 30 degree average rake reveals west directed reverse oblique slip on this segment of the fault.

Nelson and Church (1943), Keefer (1964), and Dorr and others (1977) considered the east trending segment of the New Fork fault, shown on Figure 5, to be a southeast extension of the Cache Creek thrust. They also mapped the north trending segment of the New Fork fault as the North Elbow Mountain normal fault. Later mapping by Simons and others (1988) revealed that the Cache Creek thrust turns to the south near West Dell Creek and is independent of the New Fork fault as shown on Figure 5. However, they still mapped the north trending segment of the New Fork fault as the North Elbow Mountain normal fault. Geologic mapping in this study revealed that the New Fork fault turns near The Elbow and continues northward along what has been previously mapped as the North Elbow Mountain normal fault. As shown on Figure 5, this geometry connects the New Fork fault with the east end of the Shoal Creek fault.

The connection between the New Fork fault and the previously named North Elbow Mountain normal fault is interpreted to underlie Quaternary cover immediately southwest of The Elbow (Figures 5 and 13). The west verging Elbow anticline in the hanging wall of the north trending segment of the New Fork fault is crosscut by the east-west

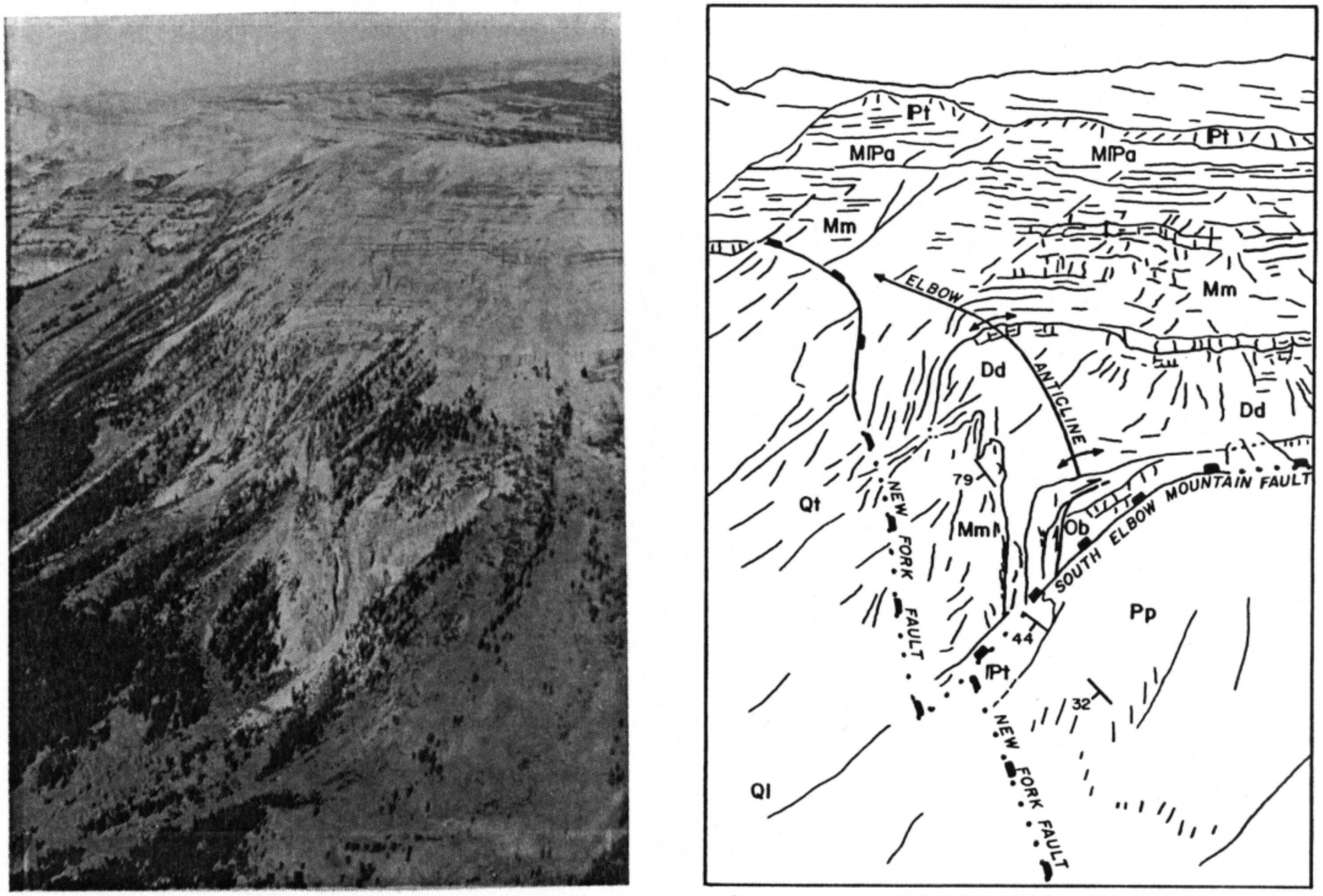

Figure 13. Photograph and line drawing of The Elbow showing Elbow anticline in the hanging wall of the north trending segment of the New Fork reverse fault, Gros Ventre Range, Wyoming. Left lateral oblique reverse slip along the South Elbow Mountain fault crosscut anticline. View is to the north. See Figure 5 for explanation of stratigraphic unit abbreviations.

trending South Elbow Mountain fault. West dipping Tensleep and Phosphoria strata immediately to the south of the severed Elbow anticline indicates that east-west fold shortening continues on the down-thrown side of the South Elbow Mountain fault. Along the east trending segment of the New Fork fault, east-west shortening was accommodated by west directed reverse oblique slip similar to that along the east trending segment of the Shoal Creek fault.

The South Elbow Mountain fault is a left lateral oblique reverse fault (or tear fault) within the hanging wall of the New Fork fault. See Figures 5, 11 E-E′, and 13. Left lateral oblique reverse slip along the South Elbow Mountain fault crosscut the Elbow anticline and allowed the hanging wall of the New Fork fault to the north to be transported about one thousand feet farther west than the hanging wall to the south.

Mapping in this study connects the New Fork and Shoal Creek faults into a single west directed reverse fault system. This fault system is characterized by west directed reverse dip slip along the north trending segments and west directed reverse oblique slip along the east trending segments of each of the two faults. As shown on Figure 5, the Shoal Creek and New Fork faults are connected at the head of Dell Creek. At this point, west directed reverse dip slip along the north trending segment of the New Fork fault was transferred to simultaneous west directed reverse oblique slip along the east trending segment of the Shoal Creek fault.

The east trending segment of the New Fork fault severs the middle early Eocene Pass Peak Formation near Jack Creek as shown on Figures 5 and 11 E-E′. Five miles to the west, undeformed Pass Peak Formation unconformably overlies Hoback strata deformed by movement along the Cache Creek thrust (Simons and others, 1988). These relationships, shown schematically on Figure 10, reveal that displacement along the Shoal Creek-New Fork fault system occurred after middle early Eocene time and after movement along the Cache Creek thrust had ceased. No sediments older than Quaternary talus and alluvium cover the traces the Shoal Creek, New Fork, and South Elbow Mountain faults so timing of movement is poorly constrained. However, Dorr and others (1977) report large angular blocks of soft Triassic sandstones incorporated into the upper Pass Peak Formation immediately south of the New Fork fault. This indicates at least some movement along the New Fork fault during middle early Eocene time. How much longer movement along the Shoal Creek-New Fork fault system continued after this time is uncertain.

Post-Laramide Extensional Faults

As shown on Figure 5, extensional faults crosscut Laramide compressional faults in the eastern Gros Ventre Range. These extensional faults do not displace any rocks younger than Triassic and are not buried by rocks older than Quaternary. Therefore, timing of movement along them is poorly constrained. The Hoback normal fault is the nearest dated extensional fault in the region. The majority of slip along this fault occurred during early Pliocene time (Olson and Schmitt, 1987). As this was a time of regional uplift and extension, it is possible that extensional faults in the Gros Ventre Range are of similar age.

CHAPTER III

THE LITHOLOGIC AND PERMEABILITY CHARACTERISTICS OF PALEOZOIC ROCKS IN THE GROS VENTRE RANGE

The purpose of this chapter is to describe the lithologic and permeability characteristics of the Paleozoic rocks in the eastern Gros Ventre Range. The Paleozoic rocks in the eastern Gros Ventre Range are divided into the Death Canyon, Madison, and Tensleep aquifers. On the mildly deformed backlimb of the range, these aquifers have small intergranular, intercrystalline, and fracture permeabilities and are separated by confining units. The small permeabilities of these aquifers in undeformed settings have little influence on ground water circulation in the eastern Gros Ventre Range.

Of much greater importance to ground water circulation are the large fracture and karst permeabilities associated with fault zones. These extremely permeable zones commonly penetrate confining layers. Therefore, they serve as large capacity vertical and horizontal pathways for ground water flow through the entire Paleozoic section.

In addition to the vertically and horizontally extensive karst systems, a surficial karst herein referred to as epikarst, has developed on the Paleozoic carbonates throughout the eastern Gros Ventre Range. Epikarst is comprised of an intricate network of solution enlarged fractures and dissolution cavities that extends downward from the surface of an exposed carbonate. See Figure 14. The depth to which epikarst extends varies between different formations, but it typically does not extend downward to the water table of the underlying regional aquifer. Epikarst is important to ground water circulation because its extreme permeability maximizes infiltration of snow melt. Epikarst temporarily stores the snow melt and discharges it from ephemeral springs before it can recharge the underlying regional aquifer.

Lithologic and Permeability Characteristics of the Death Canyon Aquifer

Where saturated, the Death Canyon Limestone Member of the Gros Ventre Formation comprises the Death Canyon aquifer. The lithologic and permeability characteristics of the Death Canyon aquifer are shown on Figure 15.

The Death Canyon Limestone is extensively karstified in the study area, particularly in the forelimb. Karstification is most noticeable where the Death Canyon Limestone is fractured and deformed along the Shoal Creek fault. Here joints, fractures, and bedding planes localize cave passages as shown in Figure 16. However, karstification in the Death Canyon Limestone is not always

Figure 14. Photograph of solution enlarged joints (fissure pits) in an epikarst zone developed in the Madison Limestone, Tosi Creek Basin, Gros Ventre Range, Wyoming. Fissure pits are 1 to 2 feet wide and more than 30 feet deep. View is to the southwest.

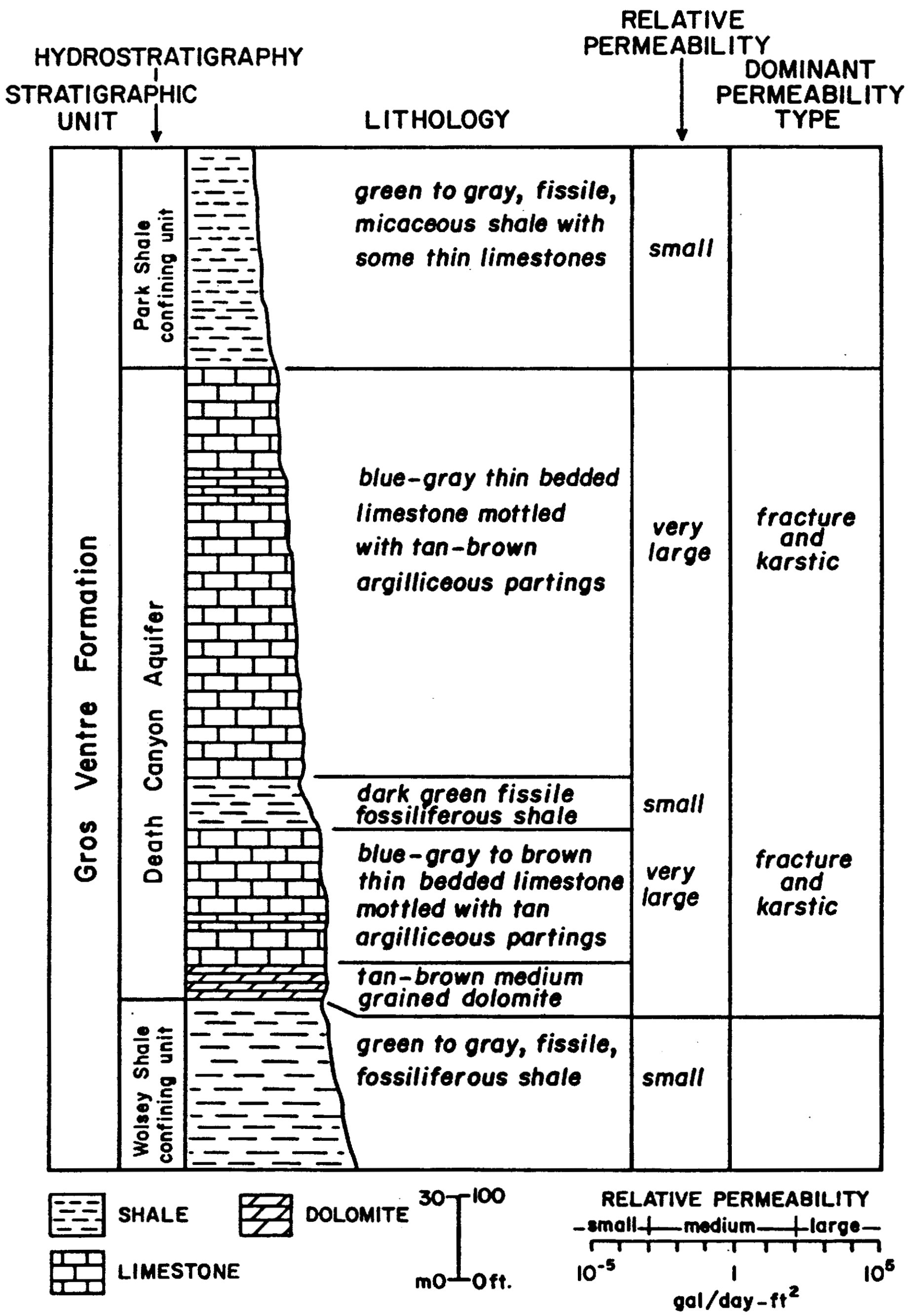

Figure 15. Stratigraphic and hydrostratigraphic column of the Death Canyon aquifer in the Gros Ventre Range, Wyoming. Column shows lithology, relative permeability, and dominant permeability type.

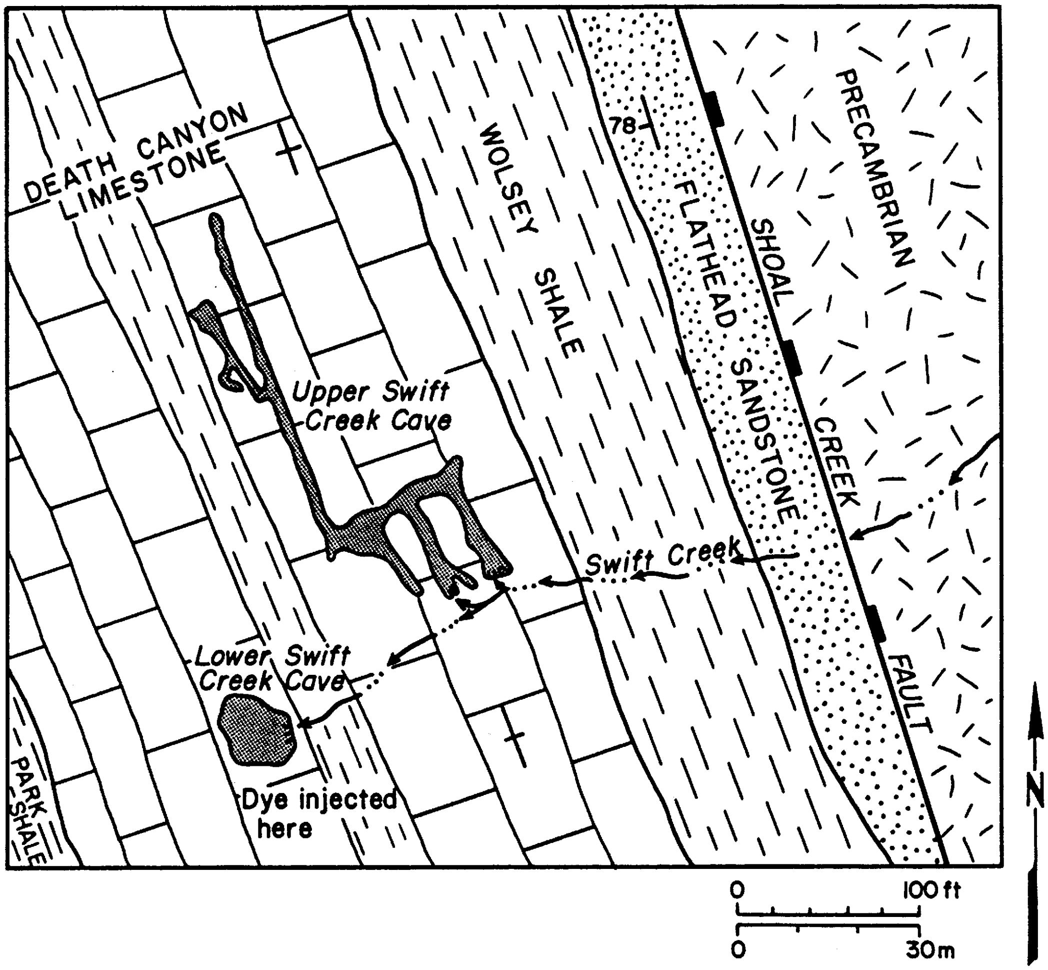

Figure 16. Geologic map of the immediate vicinity around Swift Creek caves, Gros Ventre Range, Wyoming. Cave outlines are a projection of mapped cave passages onto the land surface. Rectilinear passages are localized on joints, fractures, and bedding planes in the upturned Death Canyon Limestone near the Shoal Creek reverse fault. Modified from Hill and others (1976).

limited to fractured and deformed areas. A dye trace through karst in the Death Canyon Limestone passed with equal ease through both deformed and undeformed rock.

Lithologic and Permeability Characteristics of the Madison Aquifer

Where saturated, the Gallatin Limestone, Bighorn Dolomite, Darby Formation, and Madison Limestone comprise the Madison aquifer. See Figure 17. This section includes several thin clastic and carbonate interbeds that have small permeabilities. In undeformed setting, these interbeds behave as local confining layers within the Madison aquifer. The best examples are the clastic layers in the Darby Formation shown in Figure 17.

The most permeable part of the Madison aquifer is a 200 foot thick paleokarst at the top of the Madison Limestone. The paleokarst developed when the Madison Limestone surface was exposed over most of Wyoming and central Montana during a Meramecian (345-338 m.y.b.p.) regression of the Mississippian sea (Sando, 1988). During late Meramecian and Chesterian time (338-335 m.y.b.p.) the Amsden sea transgressed across this karst surface resulting in deposition of the beach and bar sands of the Darwin Sandstone Member of the Amsden Formation into and over the dissolution cavities in the Madison karst. The resulting sand plugs that fill solution cavities in the Madison

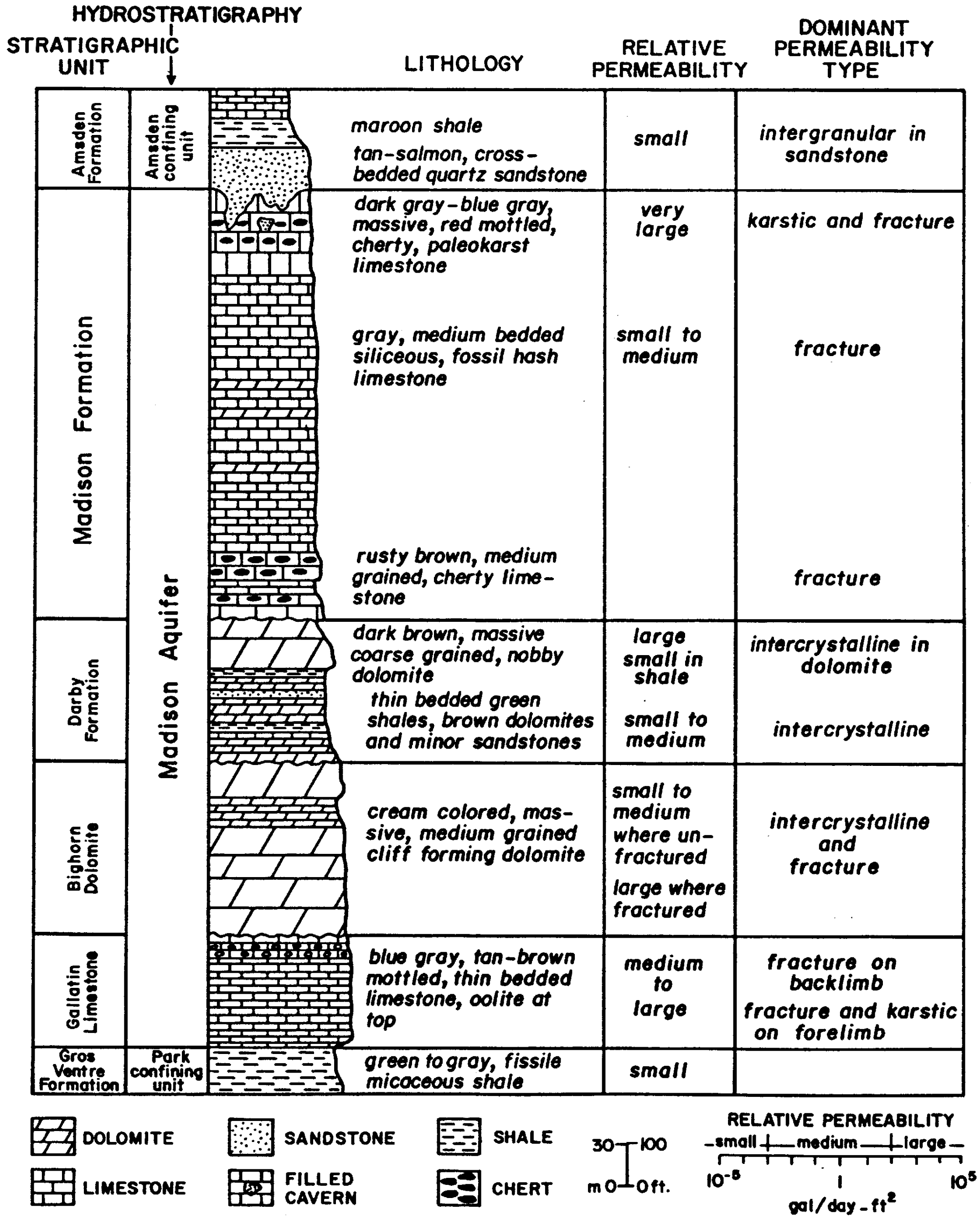

Figure 17. Stratigraphic and hydrostratigraphic column of the Madison aquifer in the Gros Ventre Range, Wyoming. Column shows lithology, relative permeability, and dominant permeability type.

paleokarst are well exposed in the Tosi Basin on the east flank of the range (Keefer, 1963; Werner, 1974). See Figure 18.

Lithologic and Permeability Characteristics of the Tensleep Aquifer

Where saturated, the Tensleep Sandstone and the lower sandstones of the overlying Phosphoria Formation comprise the Tensleep aquifer. See Figure 19.

The sandstone units in the Tensleep Sandstone are permeable whereas the intervening dolomite beds are confining layers on the mildly deformed backlimb of the eastern Gros Ventre Range. Springs issuing from each of the sandstone units discharge 0.25 to 1 ft^3/sec into backlimb streams year round.

On the forelimb, large permeabilities in the Tensleep Sandstone result from karstification of the dolomite beds and piping through the sandstone beds along fractures. Karstification and piping within the Tensleep Sandstone is often continuous with fracture and karst permeability in the Phosphoria Formation and Madison Limestone.

Figure 18. Aerial photograph of the surface of the Madison paleokarst, Tosi Creek Basin, eastern Gros Ventre Range, Wyoming. Circles are Darwin Sandstone plugs that fill paleokarst dolines. Vegetation is scarce because this very permeable surface retains little water.

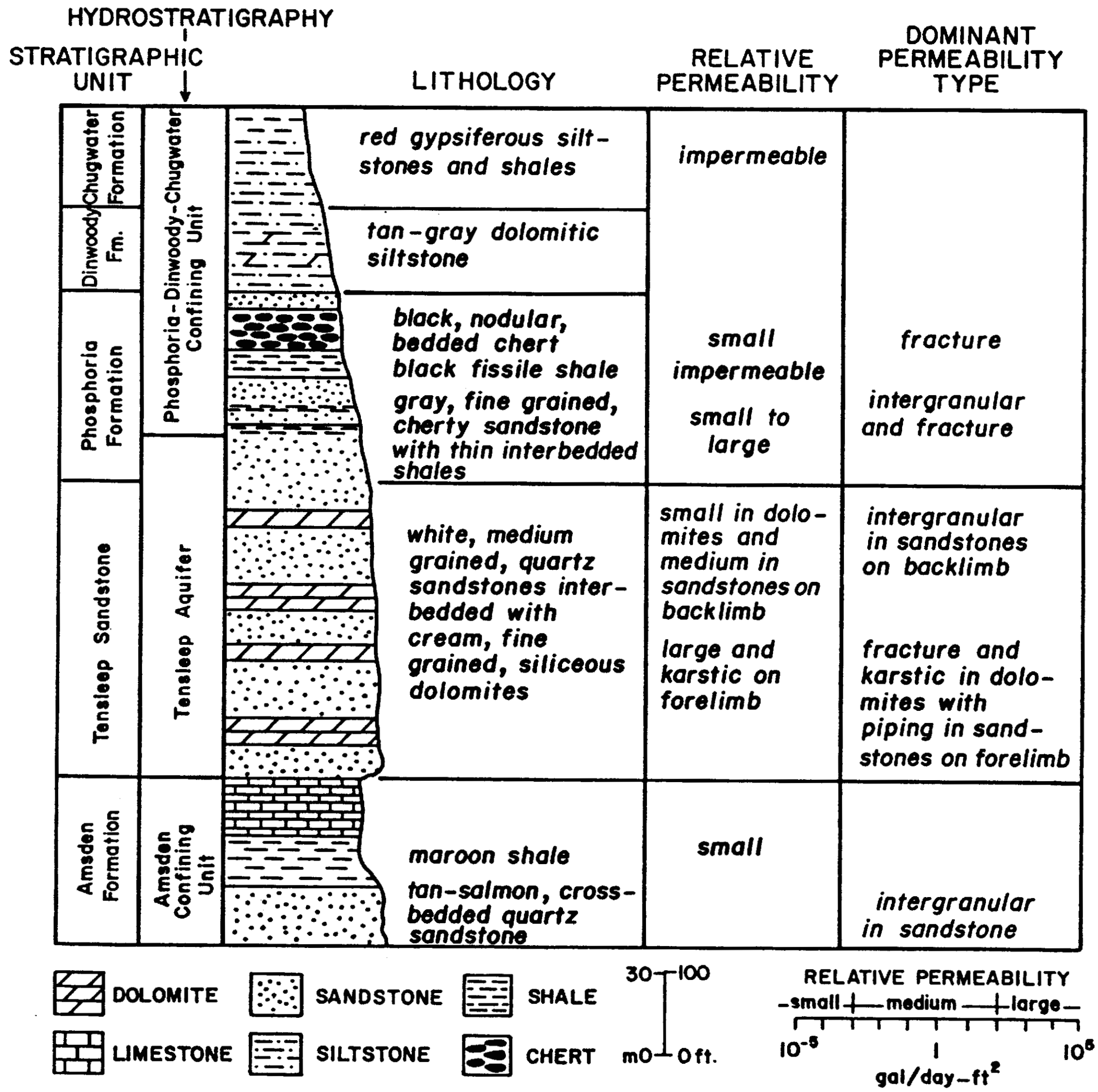

Figure 19. Stratigraphic and hydrostratigraphic column of the Tensleep aquifer in the Gros Ventre Range, Wyoming. Column shows lithology, relative permeability, and dominant permeability type.

CHAPTER IV

GROUND WATER QUALITIES IN THE PALEOZOIC ROCKS OF THE GROS VENTRE RANGE

Fifty-three water samples were collected from springs and analyzed for major ions in order to characterize water qualities in the Paleozoic rocks of the eastern Gros Ventre Range. Some springs were sampled more than once to identify seasonal variations in major ion chemistry.

Figure 20 and Appendix C show the chemical composition of ground waters from the Death Canyon Limestone. The Ca-Mg-HCO_3 dominance of these samples reflects dissolution of the Death Canyon Limestone.

Figure 21 and Appendix C show the chemical composition of ground waters from rocks comprising the Madison aquifer. The major ion chemistry of these waters is indistinguishable from that of waters from the Death Canyon Limestone. Sulfate concentrations of less than 13 mg/l in these waters reveals that there is little gypsum, either bedded or as cement, in the rocks comprising the Madison aquifer. Gypsum is reported by Wanless and others (1955) in measured sections of the Madison Limestone in Hoback Canyon twenty miles to the southwest. The small sulfate concentrations in these samples indicates that gypsum was either not deposited

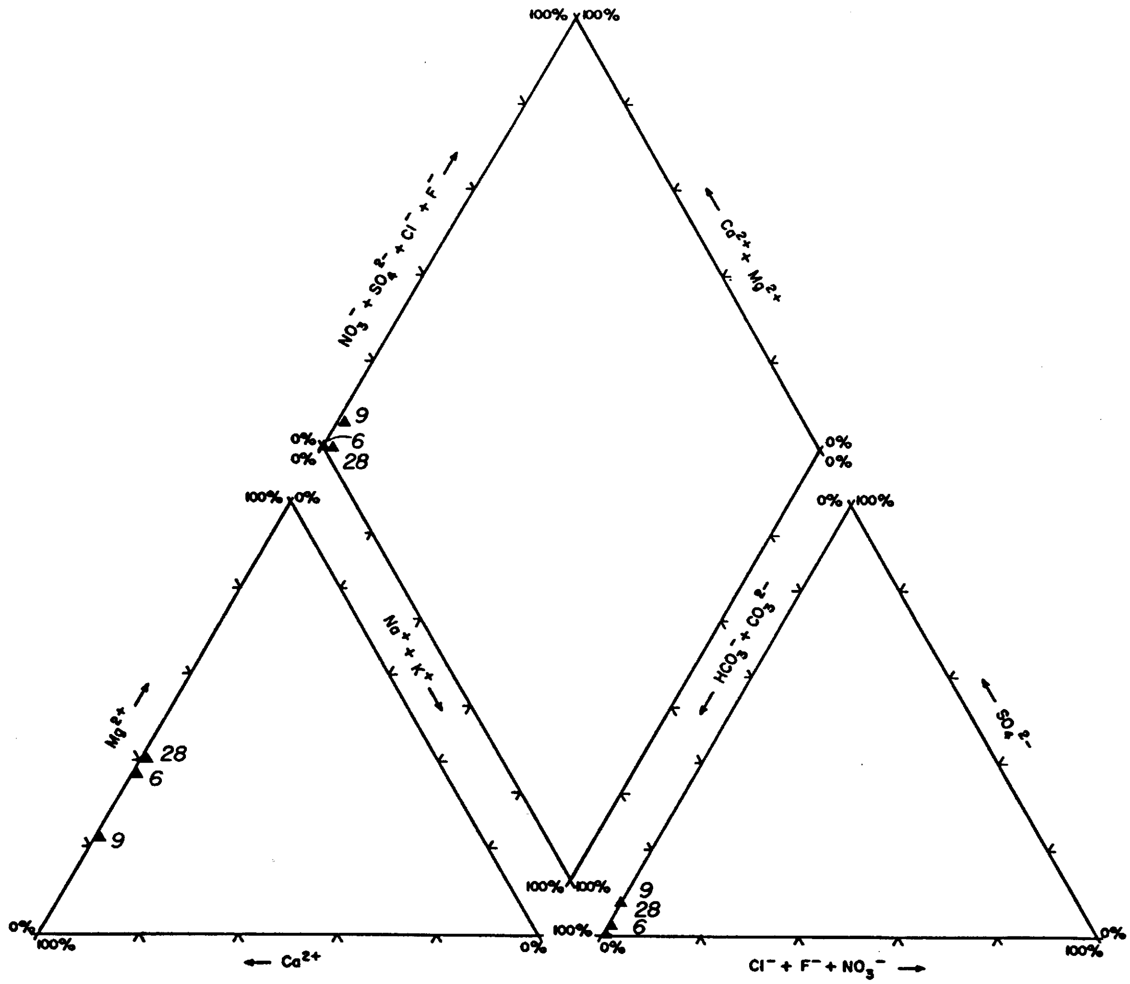

Figure 20. Trilinear diagram showing the chemical composition of ground waters from the Death Canyon Limestone Member of the Gros Ventre Formation, Gros Ventre Range, Wyoming. Numbers refer to spring locations on Figure 6 and sample analyses in Appendix C.

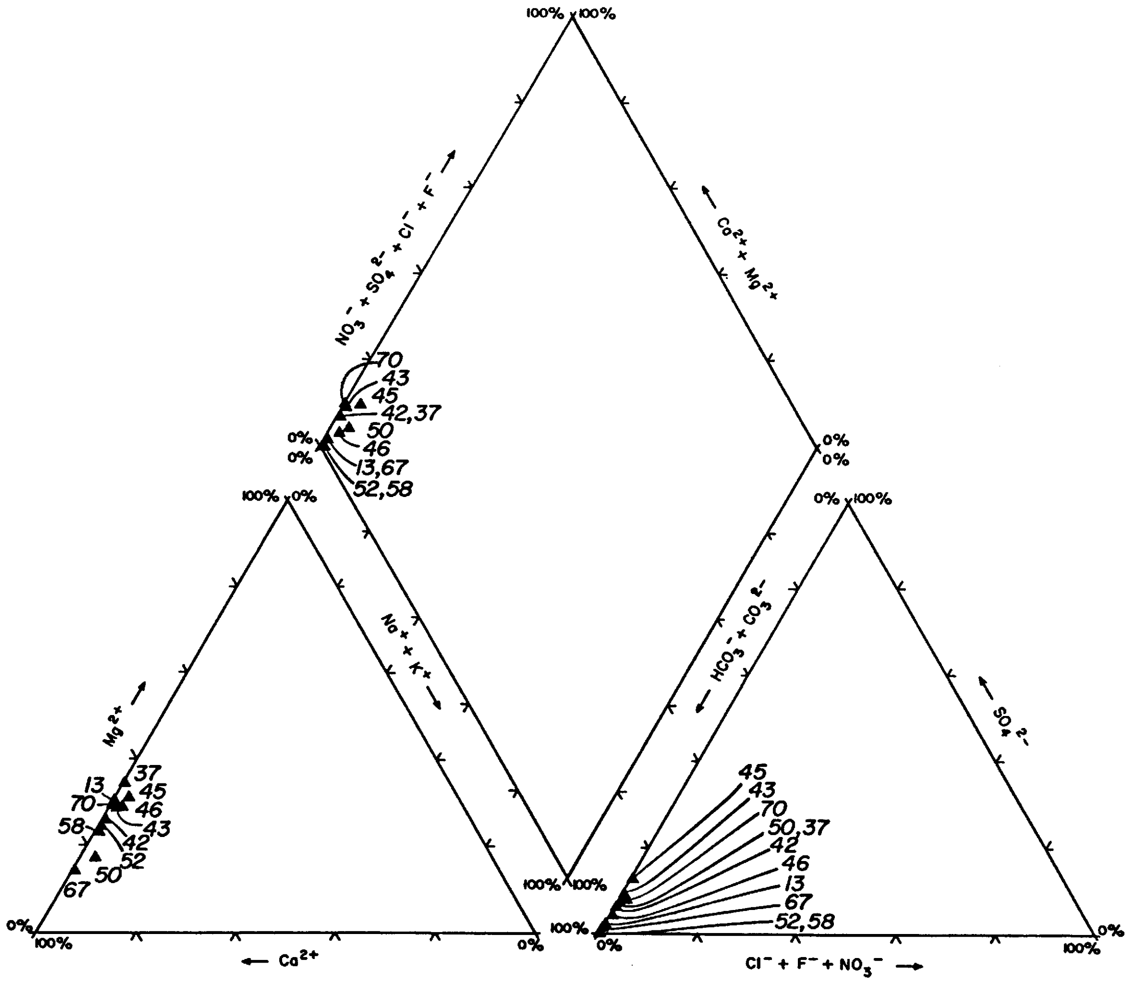

Figure 21. Trilinear diagram showing the chemical composition of ground waters from the rocks comprising the Madison aquifer, Gros Ventre Range, Wyoming. Numbers refer to spring locations on Figure 6 and sample analyses in Appendix C.

in the Madison Limestone of the Gros Ventre Range or has long since been removed by ground water.

Figure 22 and Appendix C show the chemical composition of ground waters from the Tensleep Sandstone. Increased sulfate concentrations, up to 140 mg/l, distinguish ground water in the Tensleep Sandstone from that in the rocks comprising the Madison and Death Canyon aquifers. Bedded gypsum is not reported in any Tensleep Sandstone sections measured by Wanless and others (1955) in Hoback Canyon. Therefore, sulfate in Tensleep waters is derived from dissolution of gypsum cement in the Tensleep Sandstone.

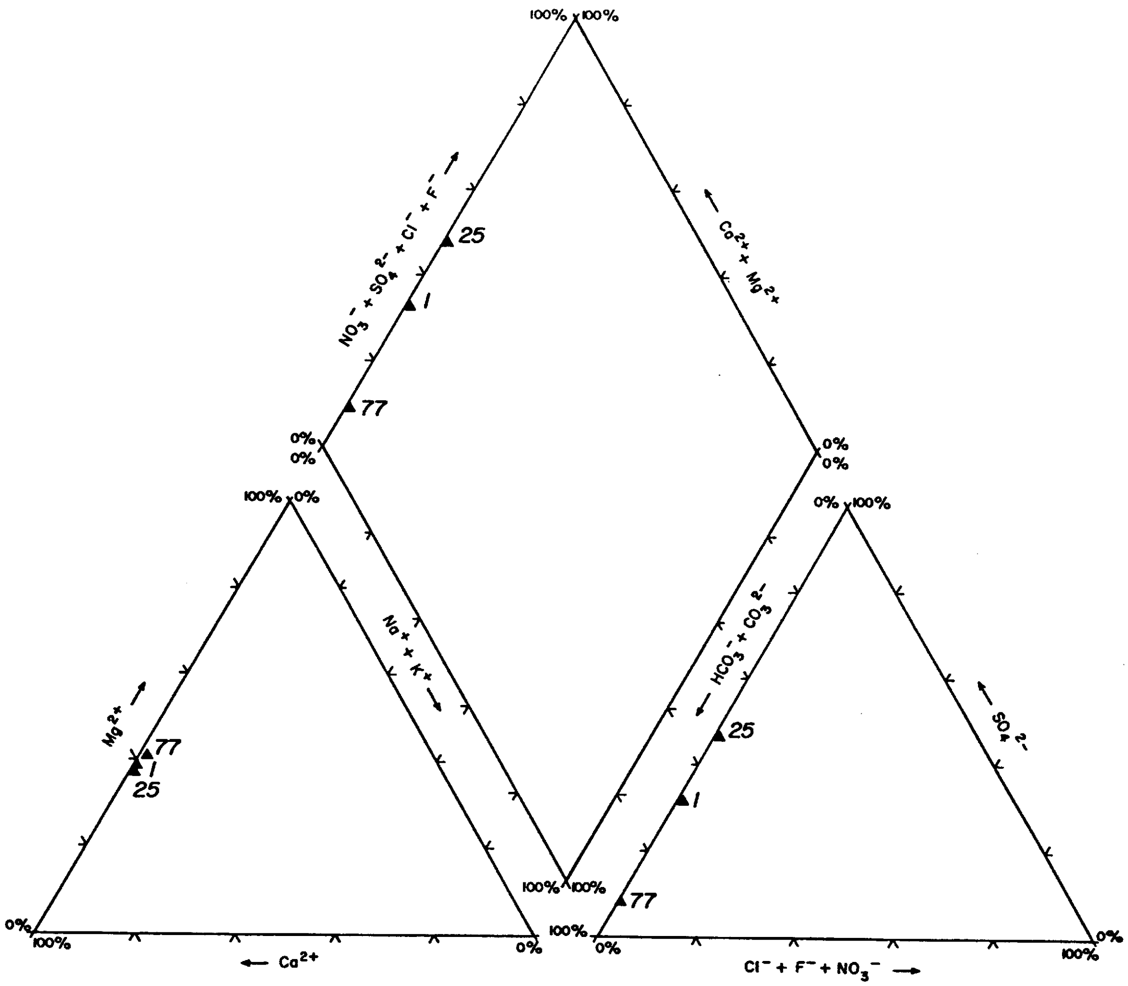

Figure 22. Trilinear diagram showing the chemical composition of ground waters from the Tensleep Sandstone, Gros Ventre Range, Wyoming. Numbers refer to spring locations shown on Figure 6 and sample analyses in Appendix C.

CHAPTER V

PERMEABILITY AND GROUND WATER STORAGE IN THE EASTERN GROS VENTRE RANGE

The purpose of this chapter is to describe the types of permeability which most influence ground water circulation and storage in the eastern Gros Ventre Range. It will be shown that the large fracture and karst permeabilities associated with fault zones and the solution enlarged fractures and dissolution cavities in epikarst zones dominate ground water circulation and storage in the range.

Water which infiltrates the Paleozoic rocks in the eastern Gros Ventre Range is stored and discharged in three ways: (1) storage and discharge from a regional aquifer, (2) storage and discharge from the myriad of interconnected caves and fractures in a deep penetrating but mostly unsaturated karst system, and (3) transient storage in and discharge from epikarst zones above the regional aquifers.

Transient storage refers to ground water temporarily stored in epikarst when the spring and summer snow melt partially saturates the epikarst zone. As shown on Figure 23, ground water in transient storage is perched in epikarst zones above the zones of saturation associated with regional aquifers. Transient storage zones are separated from the

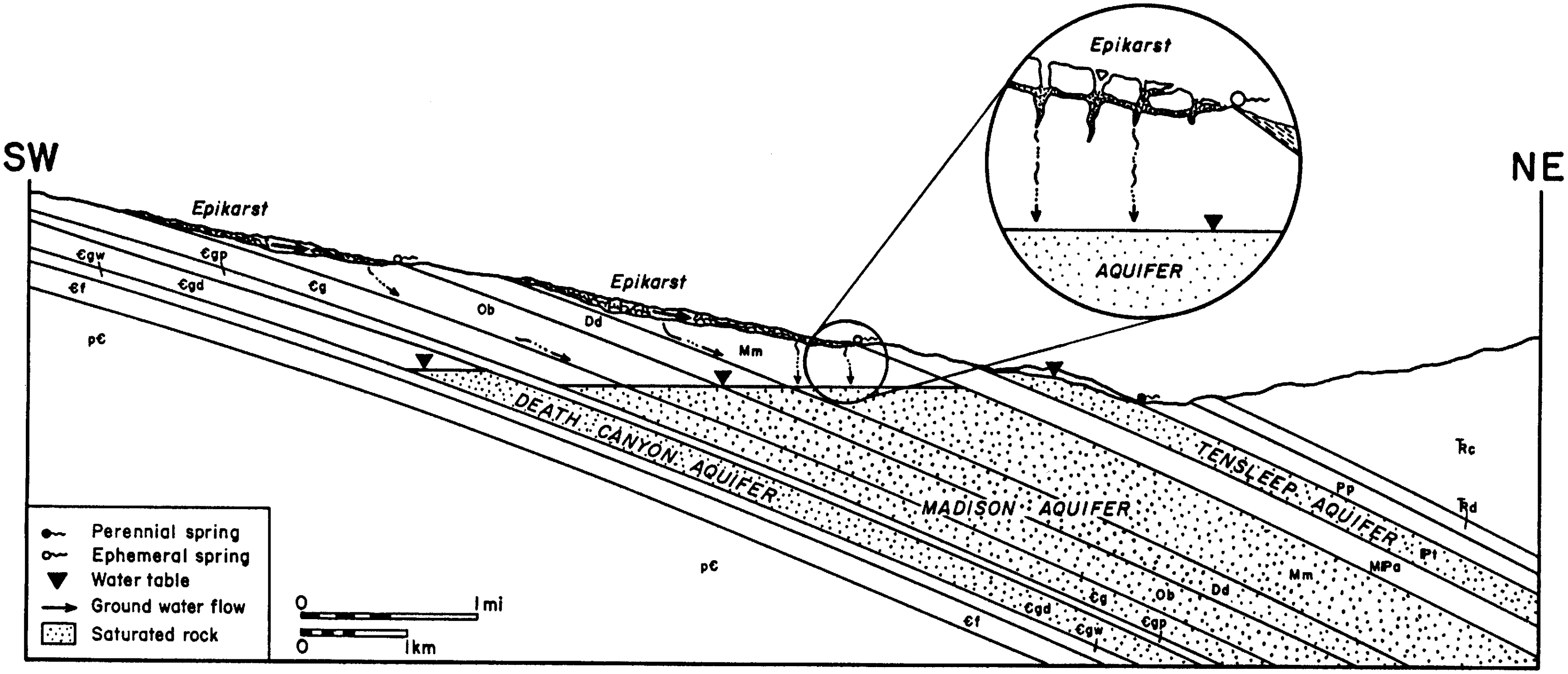

Figure 23. Schematic northeast-southwest cross section through the backlimb of the eastern Gros Ventre Range, Wyoming. Cross section shows transient storage of ground water perched in an epikarst zone above the zone of saturation associated with the underlying regional aquifer. Ground water in transient storage is discharged from ephemeral springs. See Figure 5 for explanation of stratigraphic unit abbreviations.

underlying regional aquifers by unsaturated rocks which have smaller permeabilities than the epikarst zone. The large permeabilities in the epikarst zones allow for rapid transmission snow melt to ephemeral springs. As the term transient storage implies, the ephemerally saturated epikarst drains within the annual cycle.

Permeability and Storage in Paleozoic Rocks in the Forelimb of the Eastern Gros Ventre Range

Figure 24 shows that the Paleozoic rocks on the forelimb of the eastern Gros Ventre Range were folded and fractured by movement along the Cache Creek thrust and the Shoal Creek-New Fork fault system. Movement along the Cache Creek thrust severed the Paleozoic rocks from their footwall counterparts in the Hoback Basin. As a result, the forelimb is comprised of a 1 to 2 mile wide wedge of folded and fractured Paleozoic rocks with no hydraulic connection to regional aquifers in the Hoback Basin.

Karstification and piping of fractures through the confining layers within the Paleozoic section has resulted in vertical hydraulic interconnection throughout the entire Paleozoic section in the forelimb. This allows for rapid vertical ground water flow through more than 2000 feet of unsaturated rock.

In a typical forelimb setting, snow melt and precipitation circulates downward through unsaturated

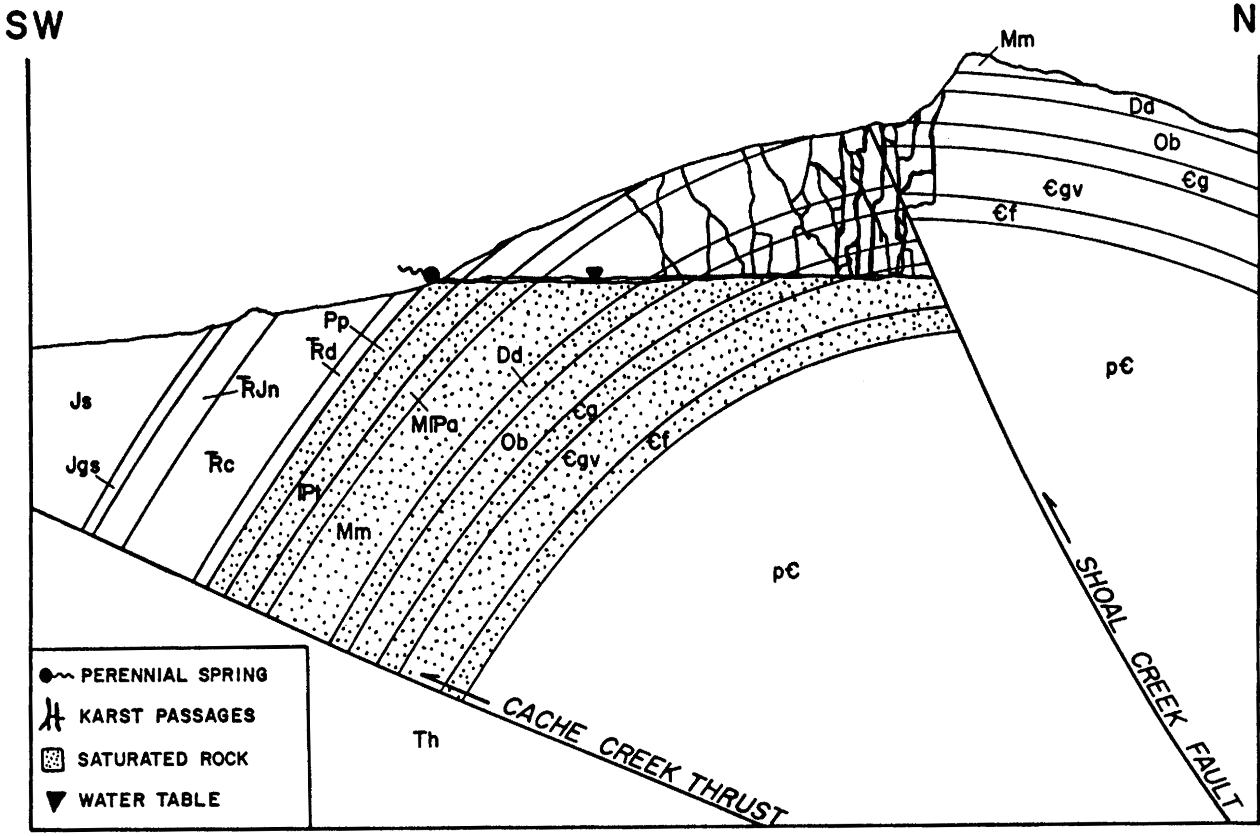

Figure 24. Schematic northeast-southwest cross section through the folded and fractured Paleozoic rocks in the forelimb of the eastern Gros Ventre Range, Wyoming. Cross section shows vertical karst passages along the Shoal Creek fault which rapidly transmit water to the underlying aquifer. The aquifer is comprised of the entire fracture integrated Paleozoic section. See Figure 5 for explanation of stratigraphic unit abbreviations.

Paleozoic rocks to an underlying fractured and karstified aquifer as shown on Figure 24. A large volume of ground water is stored in the aquifer which supplies large perennial springs. The discharges from these springs are more stable than those from any other large springs in the study area because storage in the aquifer moderates seasonal and yearly fluctuations in recharge. Consequently, springs from this part of the forelimb continue to discharge up to 18 ft^3/sec during the fall and are reliable year round sources for stream flows along the south flank of the range.

The entire Paleozoic section in the hanging wall of the Cache Creek thrust is above the water table of the regional aquifer in the Swift Creek area. Unlike most of the forelimb, snow melt and precipitation here infiltrates a deep karst system and is quickly discharged from the base of the Death Canyon Limestone without reaching an aquifer. The karst system discharges over 50 ft^3/sec from Twin springs during the peak snow melt periods. However, discharge from Twin springs decreases to about 1 ft^3/sec during fall and winter as shown on Figure 25.

Permeability and Storage in Paleozoic Rocks in the Backlimb of the Eastern Gros Ventre Range

As shown on Figure 26, the Paleozoic rocks in the backlimb of the Gros Ventre Range occur in a gently tilted, mildly deformed dip slope. In contrast to the forelimb,

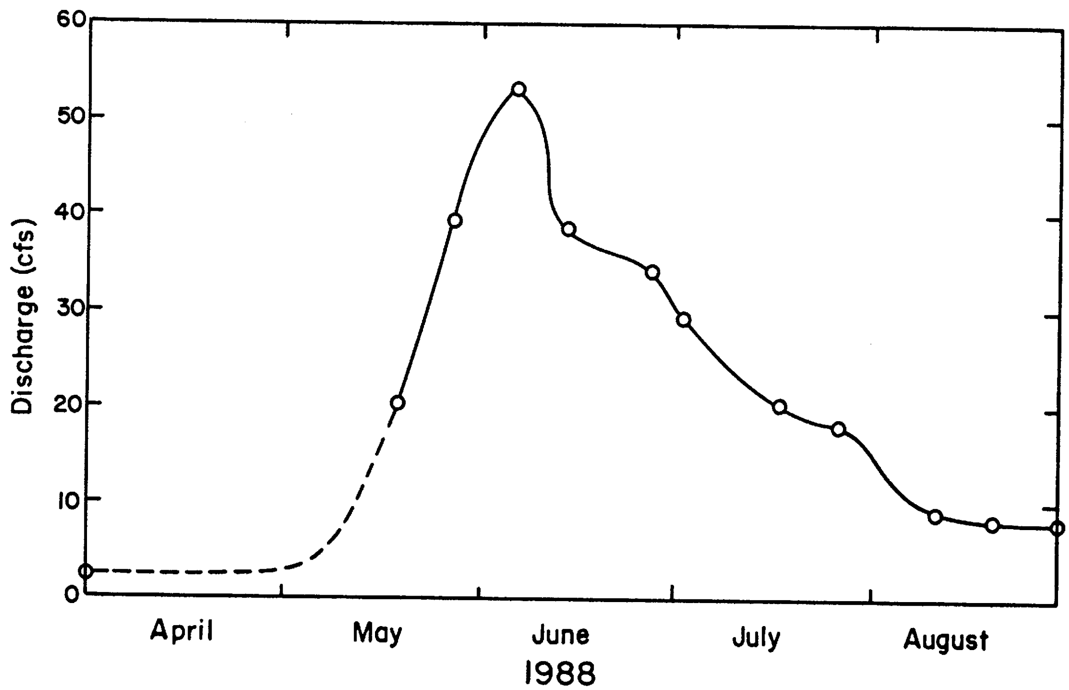

Figure 25. 1988 April through August hydrograph for Twin springs, Gros Ventre Range, Wyoming. Circles indicate measurement dates. Note that discharge is greatest during the snow melt in late May and June. April 1 measurement represents late winter flow.

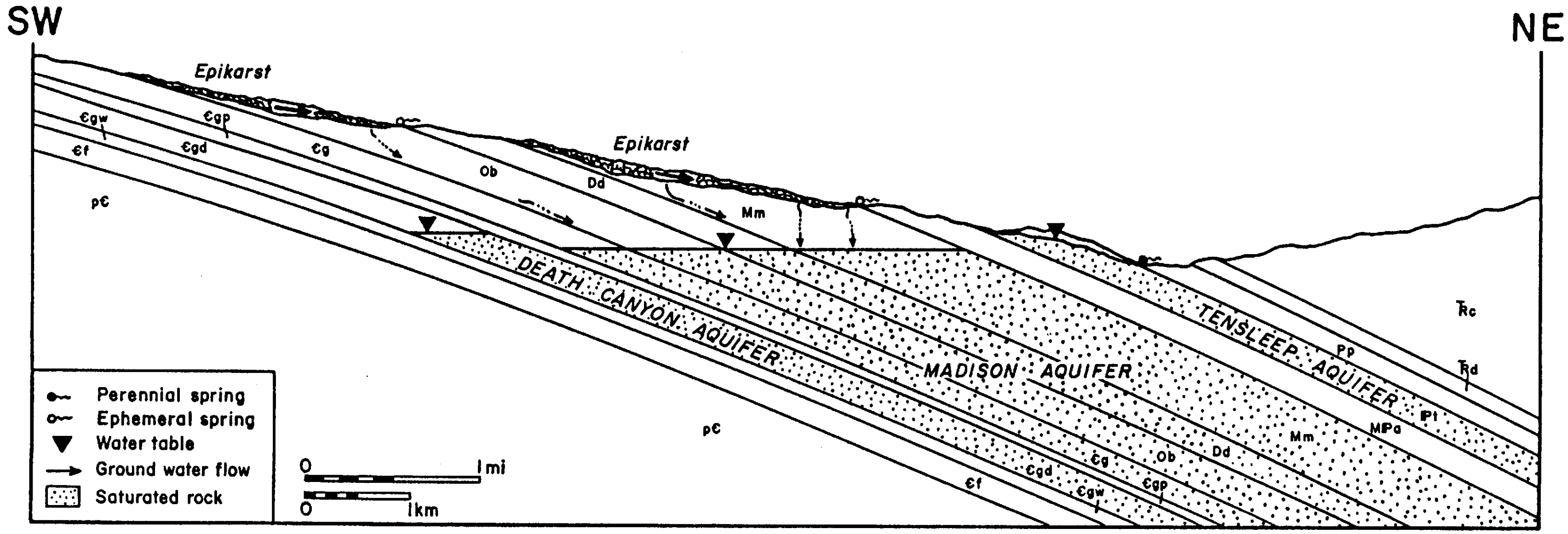

Figure 26. Schematic northeast-southwest cross section through the backlimb of the eastern Gros Ventre Range, Wyoming. Cross section shows down dip flow of ground water in temporarily saturated epikarst zones. Most ground water in the epikarst is discharged from ephemeral springs shown at toe of epikarst zones. Recharge to the underlying aquifer is small and water levels associated with it are lower than the toe of the Madison Limestone outcrop in the study area. See Figure 5 for explanation of stratigraphic unit abbreviations.

these Paleozoic rocks are stratigraphically continuous with regional aquifers in the Jackson Hole basin to the north. They also lack vertical fracture and karst permeability through the confining units as in the forelimb. Consequently, the confining units shown on Figures 15, 17, and 19 are intact and minimize vertical flow.

Epikarst zones are developed to depths up to approximately 300 feet on some backlimb exposures of Paleozoic carbonates. Water from the melting snow pack infiltrates the epikarsts and temporarily saturates parts of them. The water in transient storage within the epikarsts circulates rapidly down dip to ephemeral springs as shown on Figure 26. This water is expelled from the epikarst zones before it can recharge the underlying regional aquifer. Therefore, the saturated zones in the epikarsts are perched above the saturated zones associated with the regional aquifers. Recharge to the regional aquifers beneath the epikarsts is small and, as shown on Figure 26, the regional aquifers do not discharge.

Most of the ephemeral springs discharging from epikarst zones in the Paleozoic carbonates on the backlimb were dry by late August 1988. Therefore, it is clear that transient storage within epikarst zones in backlimb Paleozoic carbonates supplies very little water to fall and winter stream flows.

Permeability and Ground Water Storage in Precambrian Rocks in the Eastern Gros Ventre Range

Precambrian igneous and metamorphic rocks in the eastern Gros Ventre Range have small fracture permeabilities and virtually no intercrystalline permeability. Consequently, ground water infiltration is very small and the majority of snow melt on the Precambrian rocks discharges from the area directly as surface flow early in the summer.

Paleozoic rocks in the eastern Gros Ventre Range, regardless of whether they are in the forelimb or backlimb, have much larger permeabilities and ground water storage capacities than the Precambrian rocks. Consequently the Paleozoic rocks contribute much more water to fall and winter stream flows than the Precambrian rocks. Paleozoic rocks discharged approximately 1 ft^3/sec per square mile to stream flow in mid-September 1988. In contrast, Precambrian igneous and metamorphic rocks discharged less than 0.2 ft^3/sec per square mile during this same period.

CHAPTER VI

GROUND WATER SYSTEMS IN THE EASTERN GROS VENTRE RANGE

Ground water systems are defined herein on the basis of how water is stored within a body of rock. Three dominant modes are found in the eastern Gros Ventre Range: (1) water in storage in a regional aquifer, (2) water in storage in perched epikarst zones, and (3) water in transit within largely unsaturated, fractured and karstified blocks of rock.

The body of rock comprising a ground water system need not transmit all ground water to a single spring or a geographically restricted group of springs as is commonly assumed in defining a ground water basin. Rather, a ground water system includes all springs that discharge from the dominant storage mode which characterizes the system.

The eastern Gros Ventre Range is divided into four ground water systems as shown on Figure 27. The New Fork and Tensleep ground water systems include regional aquifers that discharge at springs around the flanks of the range. The Swift Creek system is an unsaturated, fractured and karstified block of Paleozoic rocks. The Gros Ventre system is characterized by transient storage within epikarst zones.

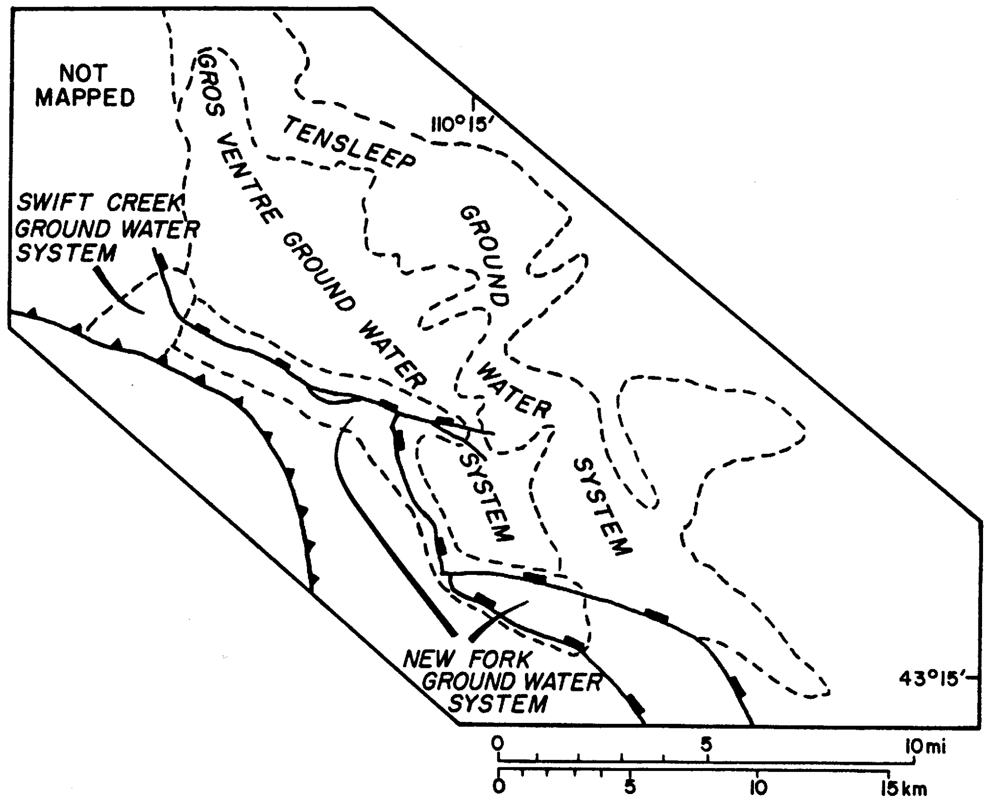

Figure 27. Map of the project area showing the principal faults and the boundaries of the four ground water systems in the eastern Gros Ventre Range, Wyoming.

The New Fork Ground Water System

The New Fork ground water system extends along the forelimb from Shoal Creek eastward to Jack Creek as shown on Figure 6. The New Fork system occupies folded and fractured Paleozoic rocks between the Shoal Creek-New Fork fault system and the Cache Creek thrust (Figure 28). Karstification and piping along fractures through the Park and Amsden confining units has hydraulically interconnected the entire Paleozoic section in the New Fork system. Where saturated the entire section behaves as a single aquifer.

Ground water stored in the aquifer in the New Fork system discharges at elevations around 8150 feet from large perennial springs at the heads of Dell, East Dell, and Jack creeks. See Figures 6 and 29. Dell and East Dell creek springs discharge near the toe of the Phosphoria outcrop whereas Jack Creek spring discharges directly along the New Fork fault. Large perennial flows from these springs reveal that they discharge ground water stored in the aquifer.

Ground water infiltrates into the Paleozoic rocks in the New Fork ground water system through fractures and swallow holes adjacent to the trace of the Shoal Creek and New Fork faults. Once in the aquifer, it flows through fractures and karst until it is discharged at the Dell, East Dell, and Jack creek springs. See Figure 6. The virtually identical elevations of these three springs reveal that they are interconnected by large fracture and karstic

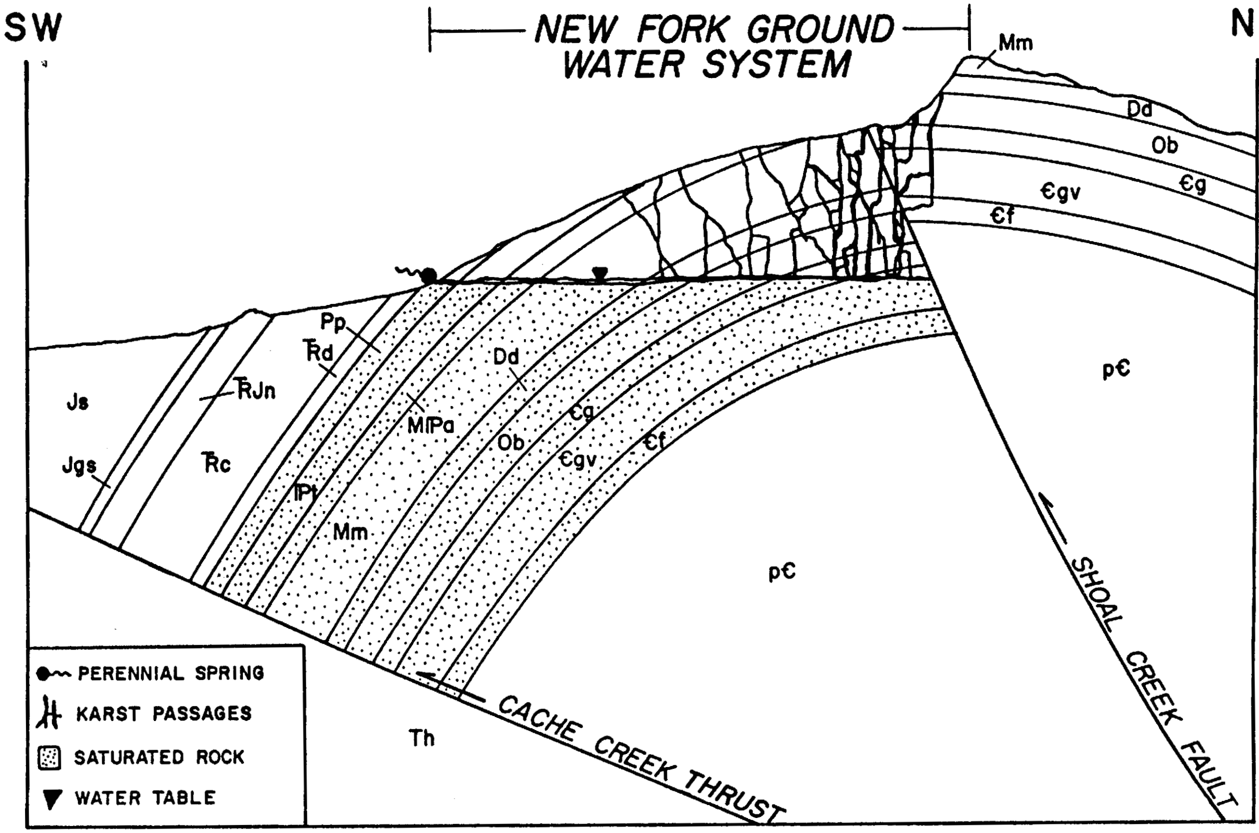

Figure 28. Schematic northeast-southwest cross section through the rocks comprising the New Fork ground water system in the eastern Gros Ventre Range, Wyoming. Cross section schematically shows the surface limits of the New Fork ground water system, the aquifer comprised of the fracture integrated Paleozoic section, and a perennial spring discharging at Phosphoria-Dinwoody contact. Spring represents both Dell and East Dell Creek springs. See Figure 5 for explanation of stratigraphic unit abbreviations.

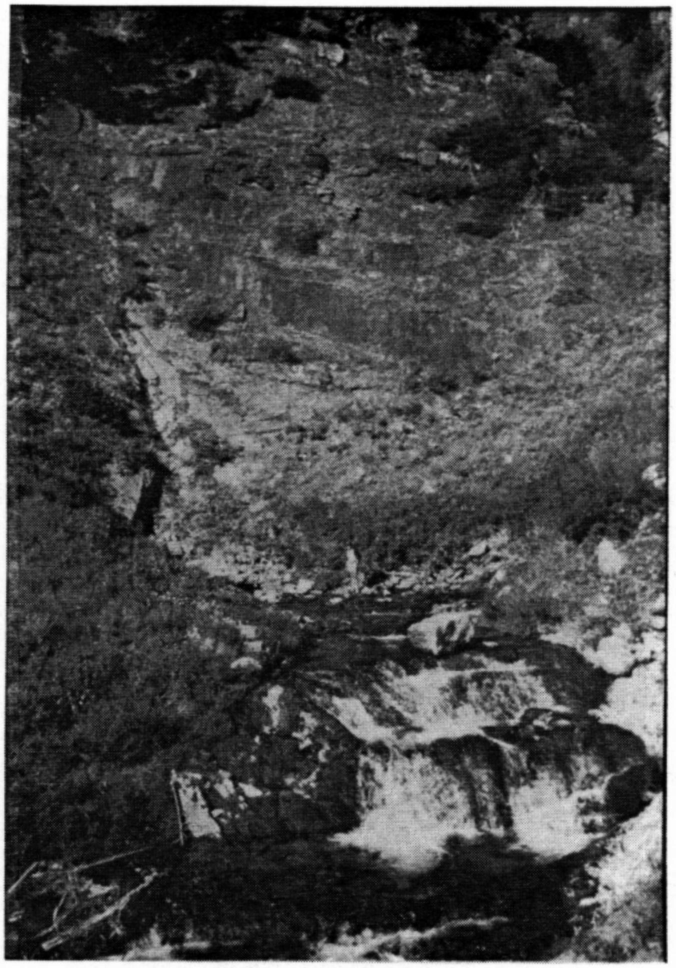

Figure 29. Photograph showing East Dell Creek spring discharging 11 ft^3/sec on August 18, 1988 from the south dipping Phosphoria Formation in the forelimb of the eastern Gros Ventre Range, Wyoming. Location of East Dell Creek spring is shown on Figure 6.

permeability along forelimb. The lateral hydraulic interconnection between the three springs supports the geometry of the New Fork fault shown on Figure 5 and discussed in chapter 2 because this geometry allows for continuous fault zone permeability between the springs.

Figure 30 reveals that water samples from the Jack, Dell, and East Dell creek springs have elevated sulfate proportions compared to water from Paleozoic carbonate rocks in other parts of the range. The increased sulfate proportions are caused by dissolution of gypsum cements in the Tensleep Sandstone which comprises part of the aquifer. The greater sulfate content of water from Jack Creek spring reflects the longer flow paths to this spring as shown on Figure 6.

The Dell Creek spring has two outlets, one approximately 100 feet in elevation above the other as shown on Figure 6. Figure 31 shows that the upper outlet of Dell Creek spring discharges more than 15 ft^3/sec during spring and early summer snow melt but decreases to a few gallons per minute by late summer. The lower outlet maintained a consistent discharge of 3 to 4 ft^3/sec over the same period.

The upper outlet serves as an overflow during snow melt when recharge to the system is greatest. The Shoal Creek fault just north of Dell Creek spring is an area of concentrated recharge to the aquifer. See Figure 6. During the spring snow melt, surface streams flow into swallow

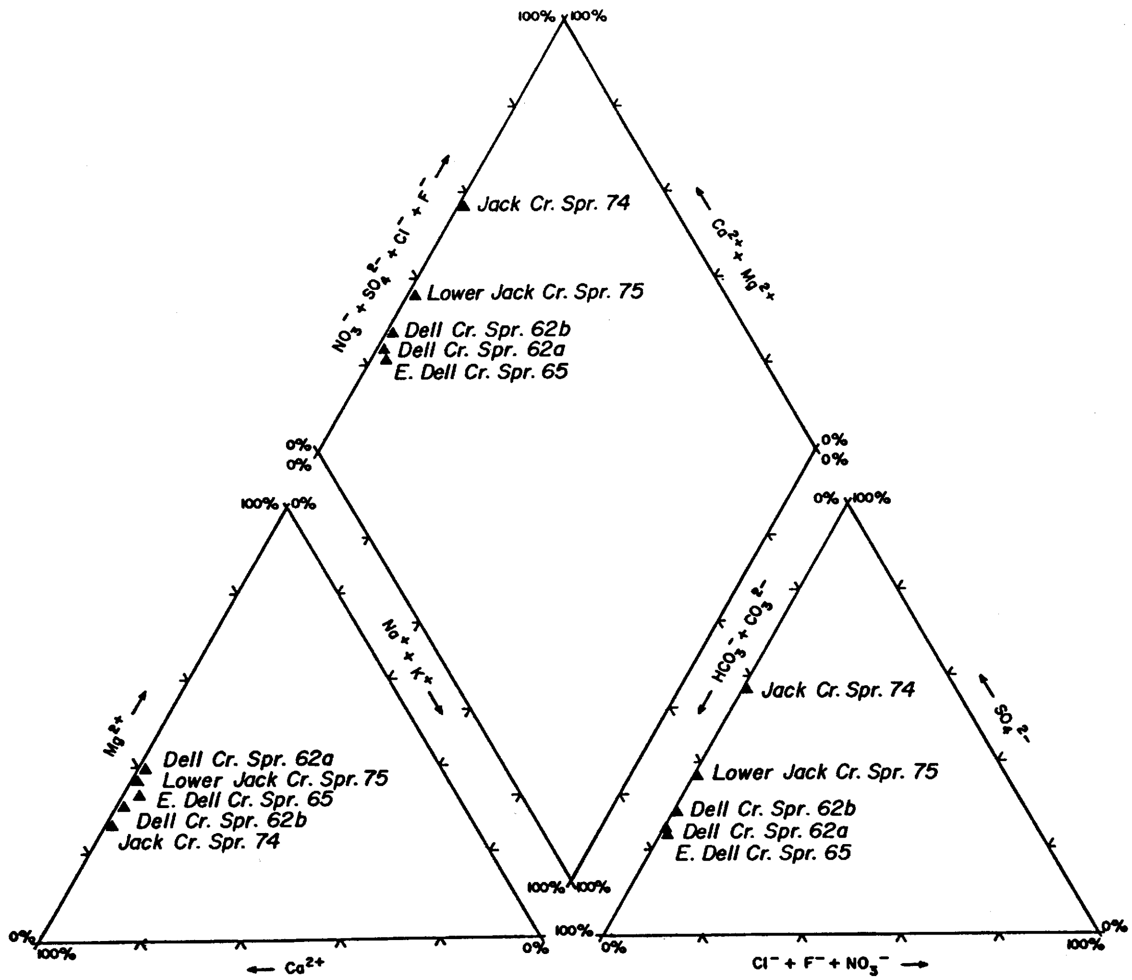

Figure 30. Trilinear diagram showing the chemical composition of ground water from Dell, East Dell, and Jack Creek springs, Gros Ventre Range, Wyoming. Numbers refer to spring locations on Figure 6 and sample analyses in Appendix C.

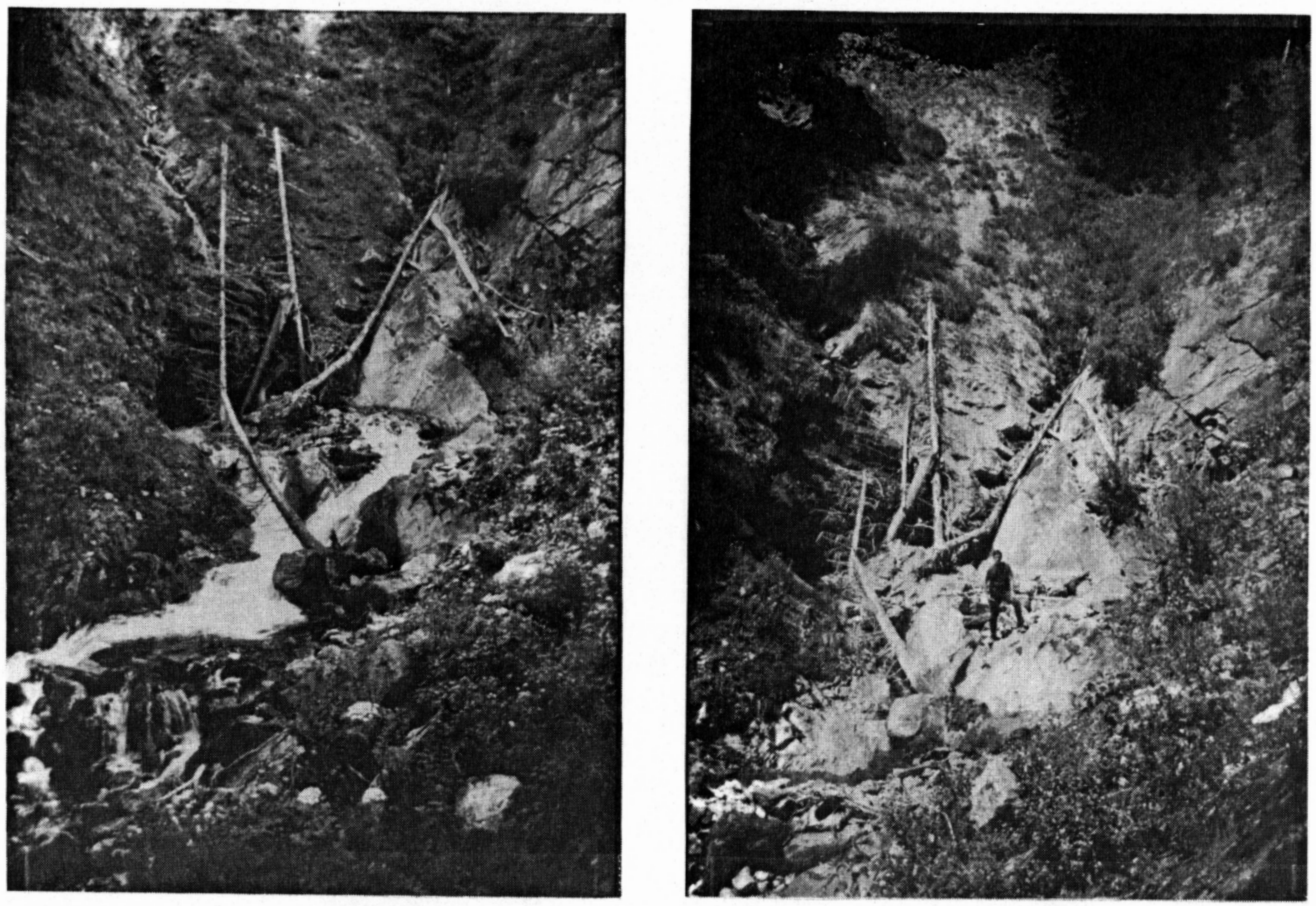

Figure 31. July 12, 1987 (left) and August 18, 1988 (right) photographs of the upper outlet of Dell Creek springs, Gros Ventre Range, Wyoming. Discharge shown in left photograph is approximately 15 ft^3/sec. Discharge shown in right photograph is less than 0.1 ft^3/sec.

holes along the fault. Recharge from snow melt raises the water table in the aquifer north of Dell Creek spring as shown in Figure 32. As a result, the hydraulic gradient steepens toward Dell Creek spring which increases the discharge from the upper outlet until the water table declines later in the summer.

The total dissolved solids concentration of water from the upper outlet varies inversely with discharge. For example, it was 93 mg/l during large discharges in June 1987, and 164 mg/l in late August 1988 when flow was only a few gallons per minute. See samples 62a and 62b in Appendix C. This dilution that accompanies large discharges indicates that snow melt infiltrating along the Shoal Creek fault zone reach Dell Creek spring in a matter of days through karst passages (Figure 32).

The Swift Creek Ground Water System

The Swift Creek ground water system, outlined on Figure 6, is comprised of a wedge of mostly unsaturated, karstified Paleozoic rocks between the Shoal Creek fault and the Cache Creek thrust. See the left side of Figure 11 B-B′. Beneath this karst system, hot, sodium-chloride rich ground water circulates through fractured Precambrian rocks along the plane of the Cache Creek thrust.

The Death Canyon Limestone is the most intensively karstified stratigraphic unit in the Swift Creek system.

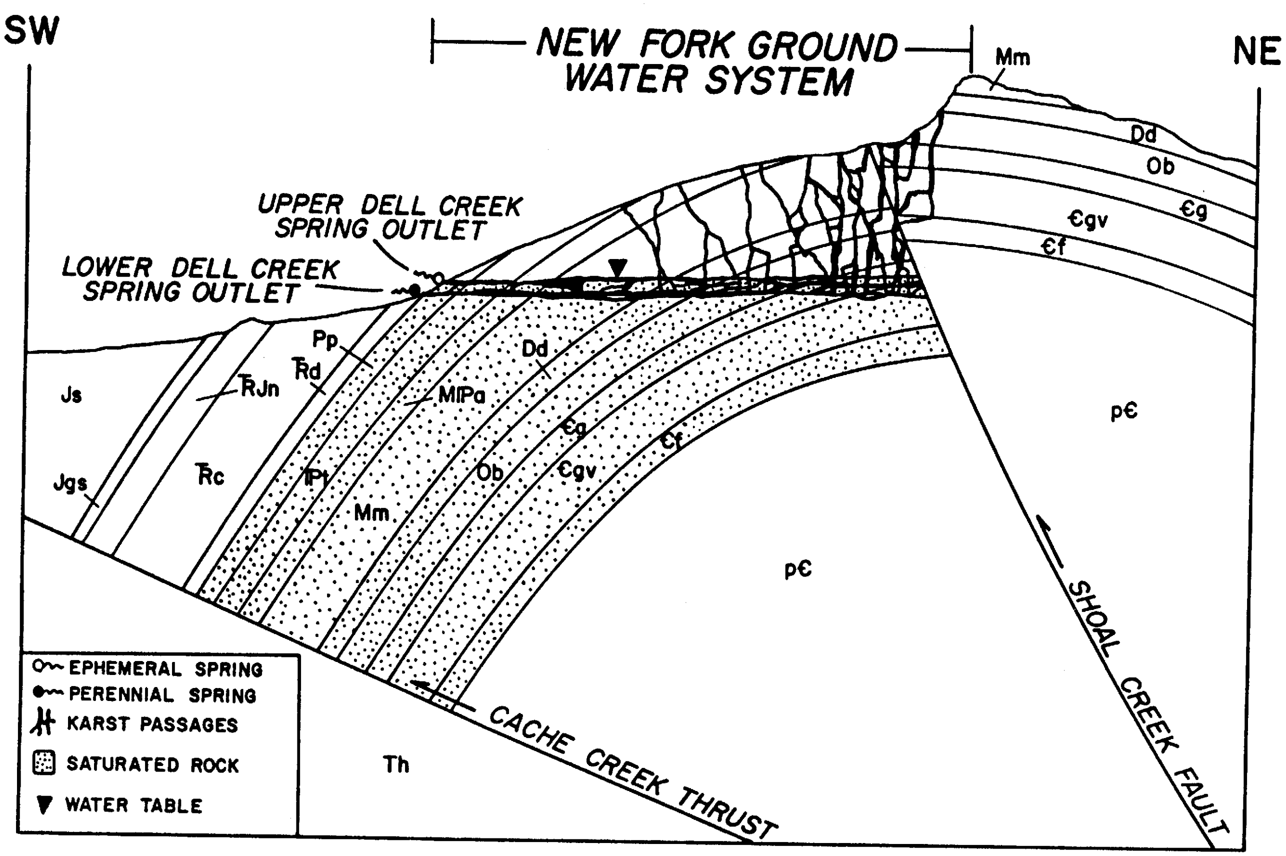

Figure 32. Schematic northeast-southwest cross section through the New Fork ground water system on the forelimb of the eastern Gros Ventre Range, Wyoming. Cross section shows the higher water table in the aquifer caused by water infiltrating along the Shoal Creek fault during the spring and early summer snow melt. Seasonally steepened hydraulic gradient towards Dell Creek springs causes discharge from upper outlet to increase. See Figure 5 for explanation of stratigraphic unit abbreviations.

Karstification is most dramatic at the head of the west fork of Swift Creek where streams that flow across the Shoal Creek fault from Precambrian terrane are lost into swallow holes such as lower Swift Creek cave shown on Figure 33.

Twin springs, shown in Figure 6, is the primary discharge point for the karst system in the Death Canyon Limestone. This spring discharges from the Cache Creek thrust indicating that karstification is continuous from the Death Canyon Limestone into and along the thrust plane to Twin springs. Discharge from this karst varies greatly through the year being largest during snow melt as shown on Figure 34.

The dye for trace 1, shown on Figure 6, was injected into lower Swift Creek cave on June 28, 1988 when flow through the karst system was large. This dye travelled three miles and dropped 2600 vertical feet to Twin springs in less than 70 hours. This corresponds to a velocity of at least 210 feet per hour which is characteristic of open channel flow through unsaturated rock. This velocity reveals that open channels are continuous between Swift Creek cave and Twin springs and that these channels remains unsaturated even during periods of greatest recharge.

In dye trace 2, dye was injected into a swallow hole in the Death Canyon Limestone along the Shoal Creek fault near the east fork of Swift Creek. See Figure 6. The dye was injected on August 5, 1988 into a 1 ft^3/sec stream entering

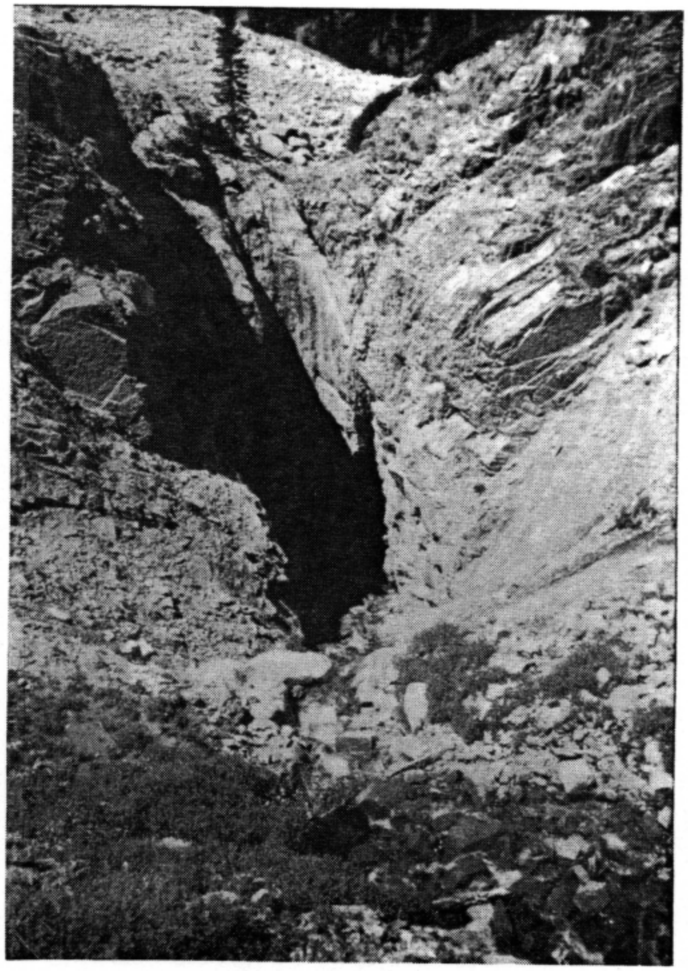

Figure 33. Photograph showing part of Swift Creek flowing into lower Swift Creek cave in the upturned Death Canyon Limestone, Gros Ventre Range, Wyoming. View is to the south.

Figure 34. April 1, 1988 (left) and June 5, 1988 (right) photographs showing water discharged from one of the two outlets of Twin springs, Gros Ventre Range, Wyoming. Discharge of less than 0.5 ft^3/sec shown on the left photograph represents late winter flow. Discharge of more than 25 ft^3/sec shown on the right photograph represents peak flow during snow melt.

the swallow hole. The dye was never recovered even through all springs in the Swift Creek ground water system were monitored for the following 2 months.

There are two possible explanations for the failure of dye trace 2. The first is that the dye is still within the karst system and transport is slow due to small late summer recharge. More plausible is the possibility that the dye dropped vertically through the unsaturated zone and then flowed eastward along the Shoal Creek fault away from any monitored springs. If this is the case, then the karst where the dye was injected is part of the New Fork ground water system as shown on Figure 6.

Ground water from both the karst system in the Death Canyon Limestone and the fractured Precambrian rock along the Cache Creek thrust discharges at Twin springs. As mentioned above, discharge of cold dilute water from the karst is greatest during snow melt. In contrast, the discharge of hot concentrated water from deep along the Cache Creek thrust is constant year round. These waters meet and mix along the Cache Creek thrust before they are discharged at Twin springs as shown in Figure 35.

The chemical composition of water discharged from Twin springs changes through the spring and summer in response to the fluctuating input from the karst system. Figure 36 shows the chemical composition of water samples taken from Twin springs through the spring and summer of 1988 compared

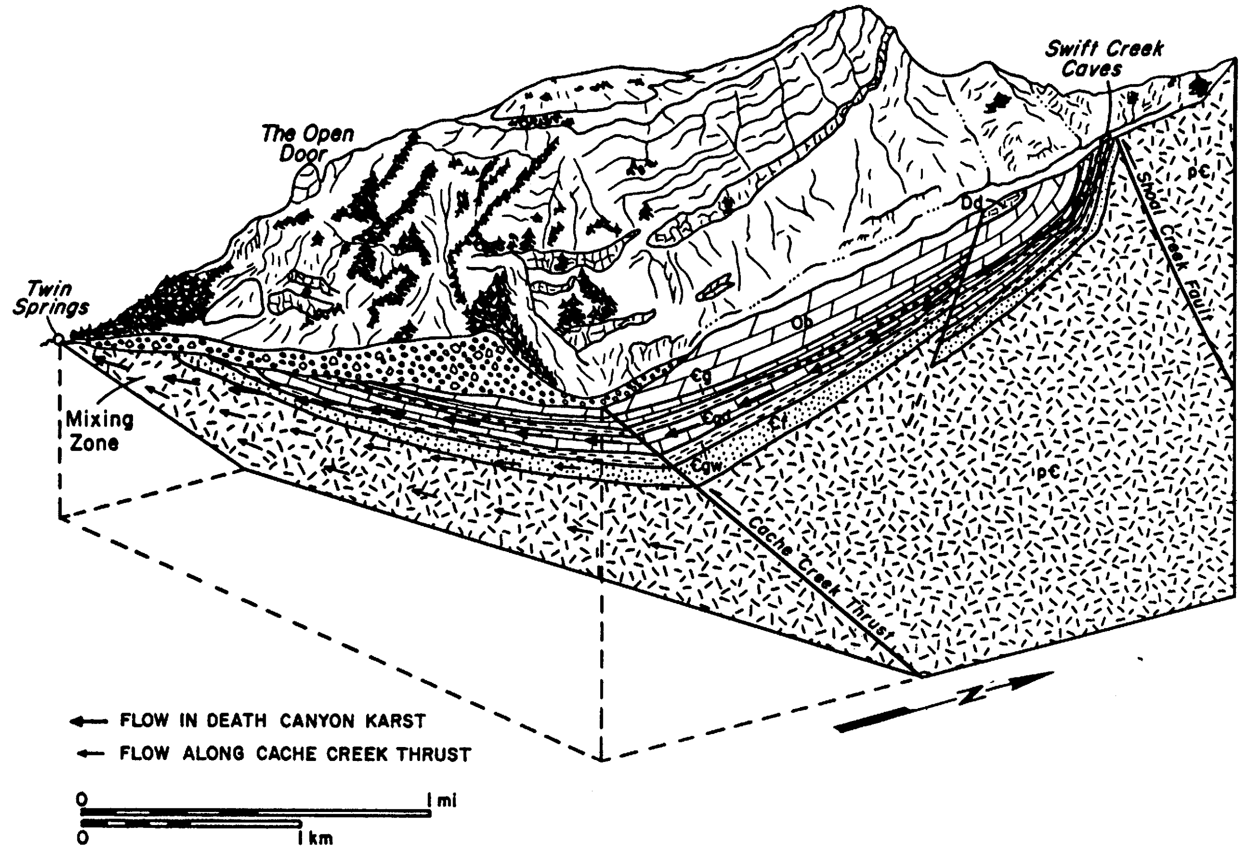

Figure 35. Schematic block diagram of part of the Swift Creek ground water system, Gros Ventre Range, Wyoming. Diagram shows the ground water flow path through the karstified Death Canyon Limestone and through fractured Precambrian rock along the Cache Creek thrust. Mixing of these waters occurs along the Cache Creek thrust before they discharge at Twin springs. See Figure 5 for explanation of stratigraphic unit abbreviations.

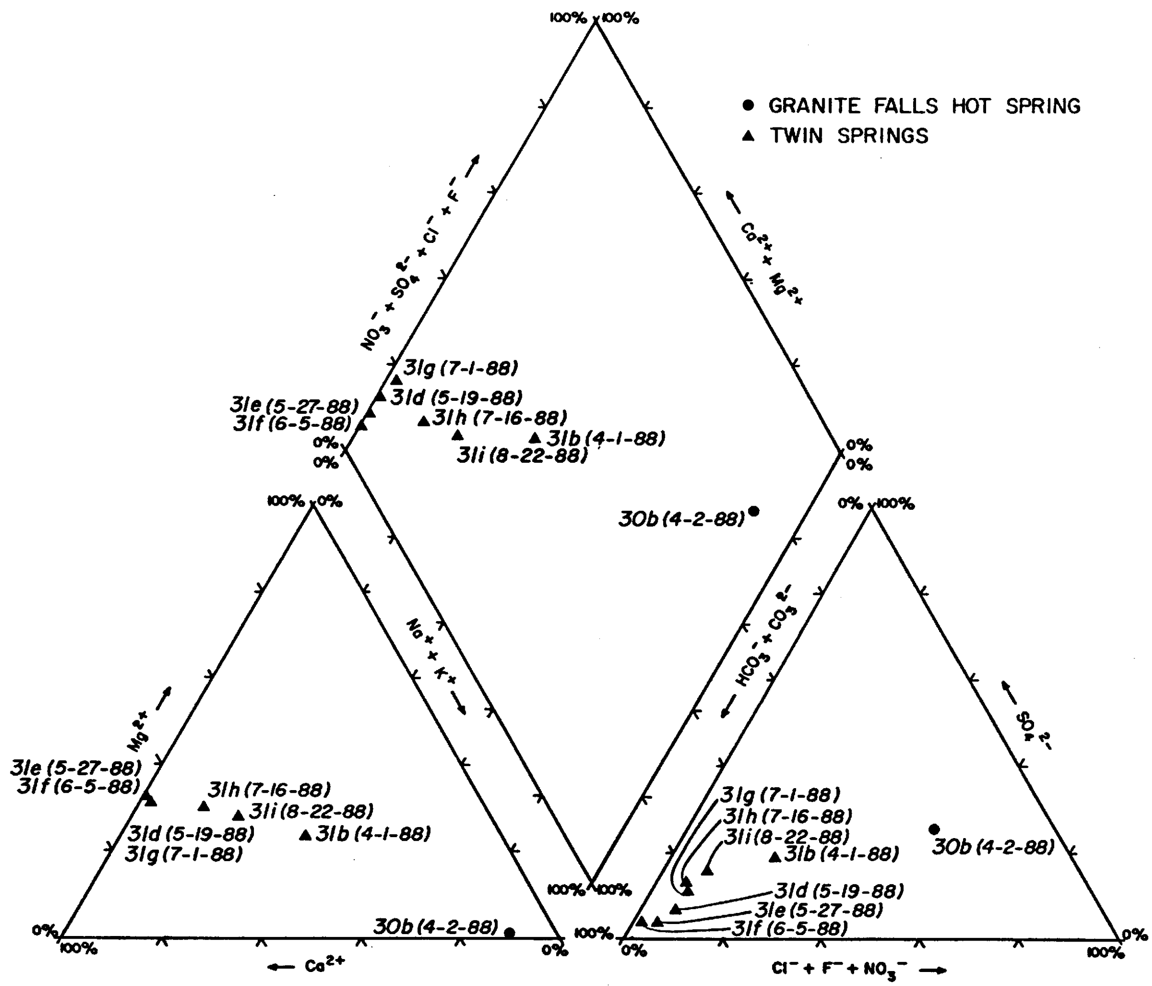

Figure 36. Trilinear diagram showing the chemical composition of seven ground water samples taken from Twin springs during the spring and summer of 1988 (triangles) and a single sample from Granite Falls hot springs (circle), Gros Ventre Range, Wyoming. Mixing of water from the Death Canyon Limestone with that from the Cache Creek thrust is revealed by the alignment of the Twin springs and Granite Falls hot springs samples. Numbers refer to spring locations on Figure 6 and sample analyses in Appendix C.

with a sample of the hot concentrated water from deep along the Cache Creek thrust, represented by Granite Falls hot springs. During peak snow melt and maximum flow in the karst system the composition of Twin springs water is nearly identical to other samples from the Death Canyon Limestone. However, as flow through the karst system diminishes through the fall and winter, the composition of Twin springs water approaches that of water from deep along the Cache Creek thrust. The temperature and chloride concentration of these waters vary inversely with discharge from Twin springs as shown on Figure 37. This reflects the decreased proportion of hot, chloride rich water present in Twin springs during periods of large flow through the karst.

The Gros Ventre Ground Water System

The Gros Ventre ground water system is comprised of all rocks from the base of the Death Canyon Limestone to the top of the Madison Limestone on the backlimb of the eastern Gros Ventre Range. As shown in Figures 6 and 38, these formations are exposed as broad dipslopes dipping between 5 and 15 degrees northeast into the Jackson Hole Basin.

The thickest and most permeable epikarst zones in the eastern Gros Ventre Range have developed on outcrops of the Madison Limestone and Bighorn Dolomite in the Gros Ventre system. Epikarst at the top of the Madison Limestone extends downward 300 feet or more and is comprised of

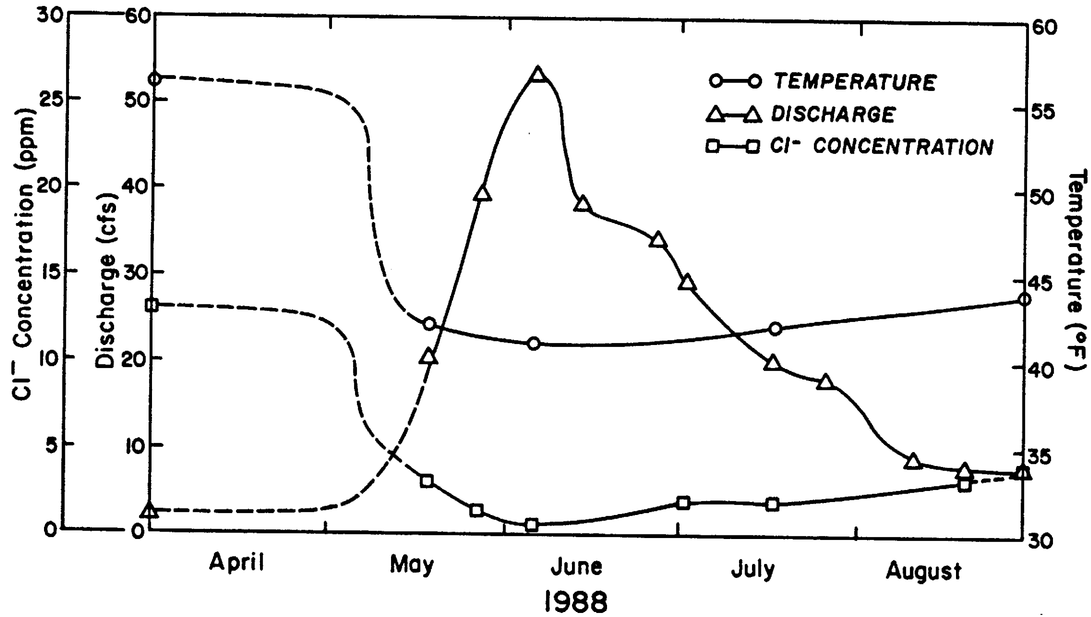

Figure 37. Graph of chloride concentration, discharge, and temperature versus time during spring and summer, 1988 for Twin springs, Gros Ventre Range, Wyoming. Graph shows smallest chloride concentrations and temperatures during the period of greatest discharge from Twin springs. Circles, squares, and triangles indicate measurement dates.

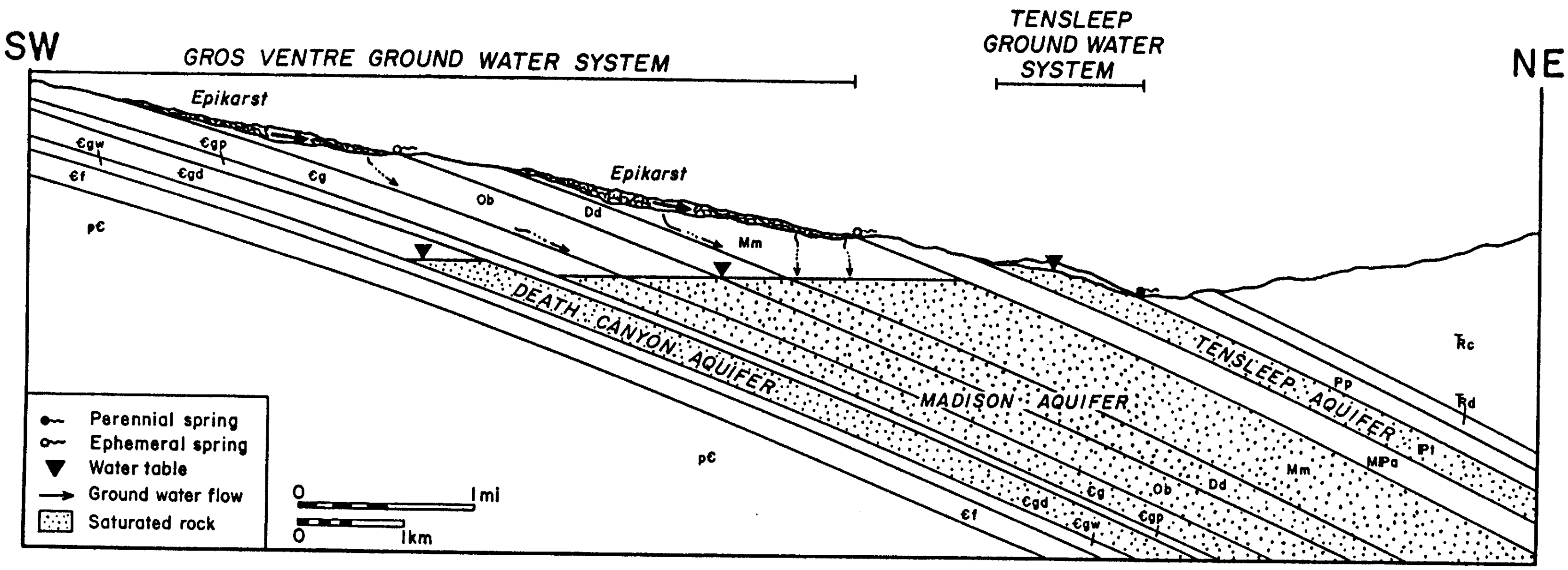

Figure 38. Schematic northeast-southwest cross section through the backlimb of the eastern Gros Ventre Range, Wyoming. Cross section shows the limits of the Gros Ventre and Tensleep ground water systems. Note that the water table of the Madison aquifer is lower than the lowest outcrop of the Madison Limestone and is also lower than water levels in the Tensleep aquifer. See Figure 5 for explanation of stratigraphic unit abbreviations.

solution enlarged joints and reexcavated paleokarst. Epikarst in the Bighorn Dolomite is characterized as a network of solution enlarged joints as shown on Figure 39. Nearly all precipitation and snow melt on these outcrops infiltrates into the epikarst.

Dye trace 3, shown on Figure 6, passed through the Madison epikarst in the upper Clear Creek drainage shown in the photograph on Figure 40. The dye travelled one mile and dropped 800 feet to a spring in less than 10 hours. The same dye infiltrated back into down gradient epikarst zones and was recovered again at several more springs farther downstream in the Clear Creek drainage.

The rapid travel times demonstrated by trace 3 reveal the enormous permeability within the Madison epikarst zone. Furthermore, the dye spread laterally to several springs downhill revealing that ground water flows through a network of interconnected karstified fractures in the Madison epikarst rather than through a single cave.

Transient storage of ground water in epikarst only can maintain spring flows for two or three months after snow melt owing to the large permeabilities which allow the zones to drain. Springs discharged as much as 10 ft^3/sec from epikarst zones in the Gros Ventre system during the spring snow melt of 1988 but most of these were dry by late August, 1988. Consequently, transient storage in epikarst contributes very little water to fall and winter stream

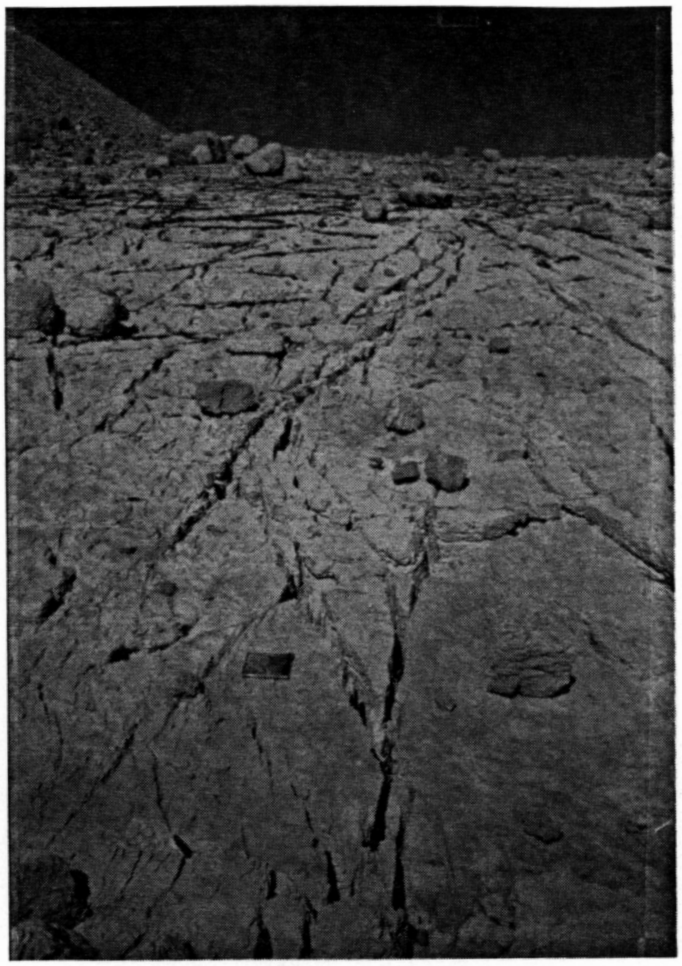

Figure 39. Photograph showing solution enlarged joints in an epikarst zone in the Bighorn Dolomite, Clear Creek drainage, Gros Ventre Range, Wyoming. Map case is 10 inches square. Solution enlarged joints are more than 20 feet deep. View is to the southwest.

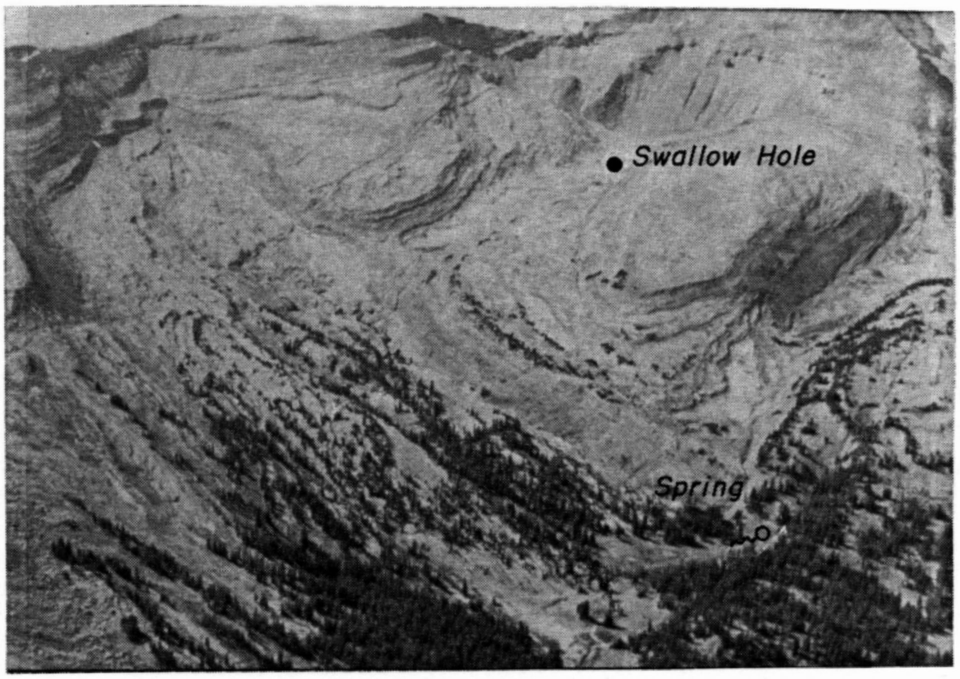

Figure 40. Aerial photograph showing the site of dye trace 3 through an epikarst zone in the Madison Limestone, Clear Creek drainage, Gros Ventre Range, Wyoming. Dye was introduced into a swallow hole shown in the upper part of the photograph and was recovered at the spring shown in the lower right corner after 10 hours. The distance of dye trace is one mile and the vertical drop is 800 feet.

flows on the backlimb of the eastern Gros Ventre Range. As shown in Appendix B, all springs in the Gros Ventre ground water system have the recession characteristics expected of transient storage in epikarst.

The water table of the regional Madison aquifer in the backlimb is lower than the lowest outcrop of the Madison Limestone and lower than the water table of the overlying Tensleep aquifer. See Figure 38. This relationship can also be detected in the Jackson Hole Basin to the north. Formation pressure data from drill stem tests in the Clayton Williams 24-1 Lightning Creek oil well (42N-113W-24) 8 miles north of the study area shows that the potentiometric surface of the Madison aquifer is 85 feet lower than that of the overlying Phosphoria Formation.

Therefore, as opposed to the regional aquifer in the forelimb, the regional Madison aquifer does not discharge ground water into backlimb streams within the project area. The lack of large perennial springs like those that discharge from the aquifer in the forelimb attests to this fact. As a result, fall and winter stream flows are much smaller on the backlimb than on the forelimb and are sourced primarily from the Tensleep ground water system.

Several lakes in the Gros Ventre ground water system occupy closed depressions and have no surface outlets. Water in them drains through the lake bottom into the underlying carbonates. Such lakes are usually perched at the contact between a confining layer and the epikarst zone of an underlying carbonate sequence as shown on Figure 41. Ground water discharges from the epikarst into the lake. Silt on the lake floor forms a semipermeable layer which slowly leaks water into the underlying rock.

The largest internally drained lakes in the Gros Ventre system are Lunch Lake and The Six Lakes. Both are perched at the contact between the Madison Limestone and overlying Amsden Formation. As shown in the photographs on Figure 42, water levels in these lakes drop dramatically between spring and fall. The lost water recharges the underlying regional Madison aquifer as shown on Figure 41.

The potentiometric surface associated with the regional Madison aquifer on the north flank of the Gros Ventre Range slopes toward the northwest. Ground water which reaches the Madison aquifer from carbonate outcrops on the backlimb flows northwestward out of the study area as shown in Figure 6. Where this water discharges is unknown.

The Tensleep Ground Water System

The Tensleep ground water system is comprised of the Tensleep Sandstone on the backlimb of the eastern Gros Ventre Range as shown on Figures 6 and 38. In this system, ground water is stored in the Tensleep aquifer which discharges near the lowest Tensleep outcrops on the backlimb.

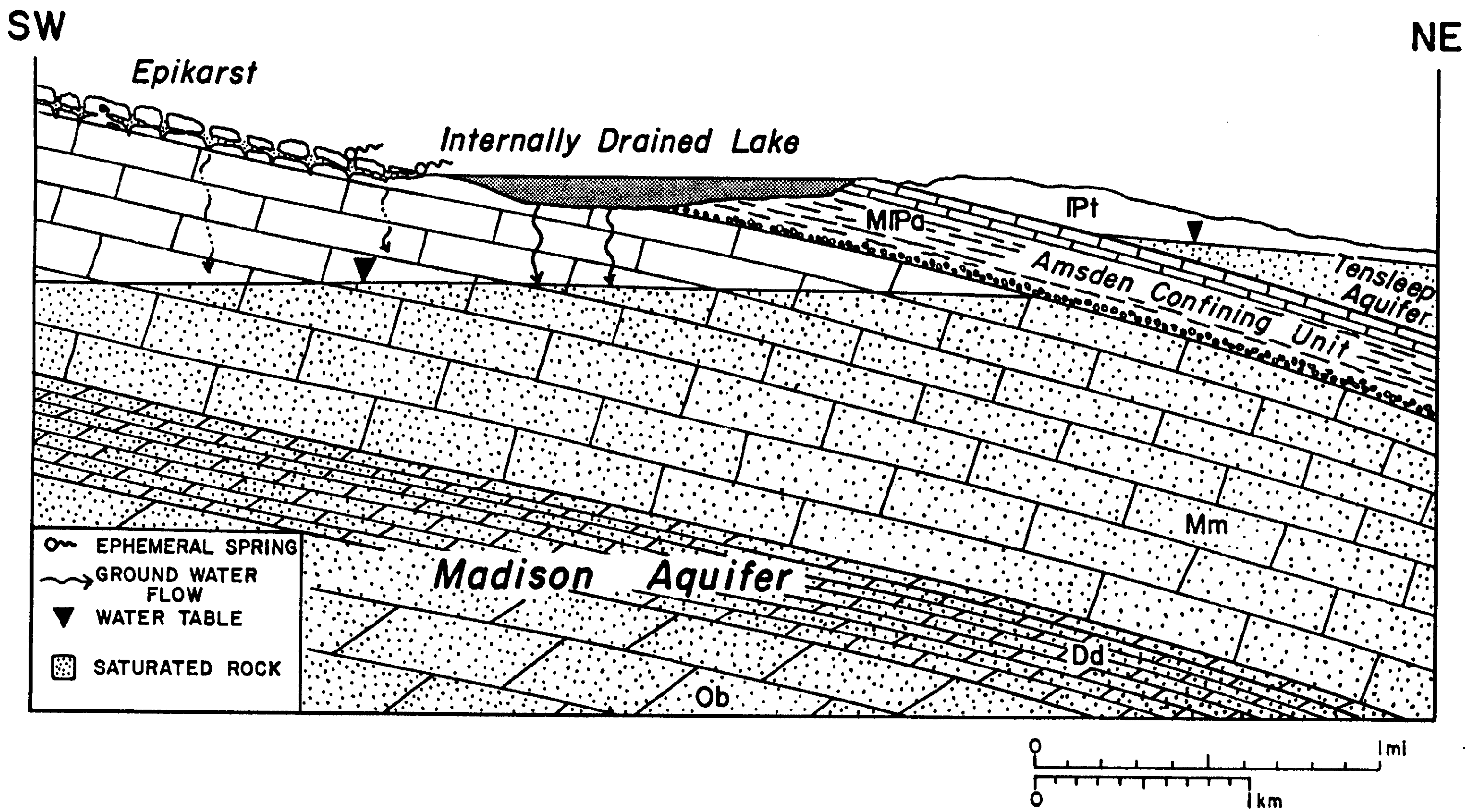

Figure 41. Schematic northeast-southwest cross section through an internally drained lake localized on the contact between the Madison Limestone and the Amsden Formation, Gros Ventre Range, Wyoming. Cross section shows leakage through the lake bottom which slowly recharges the underlying Madison aquifer.

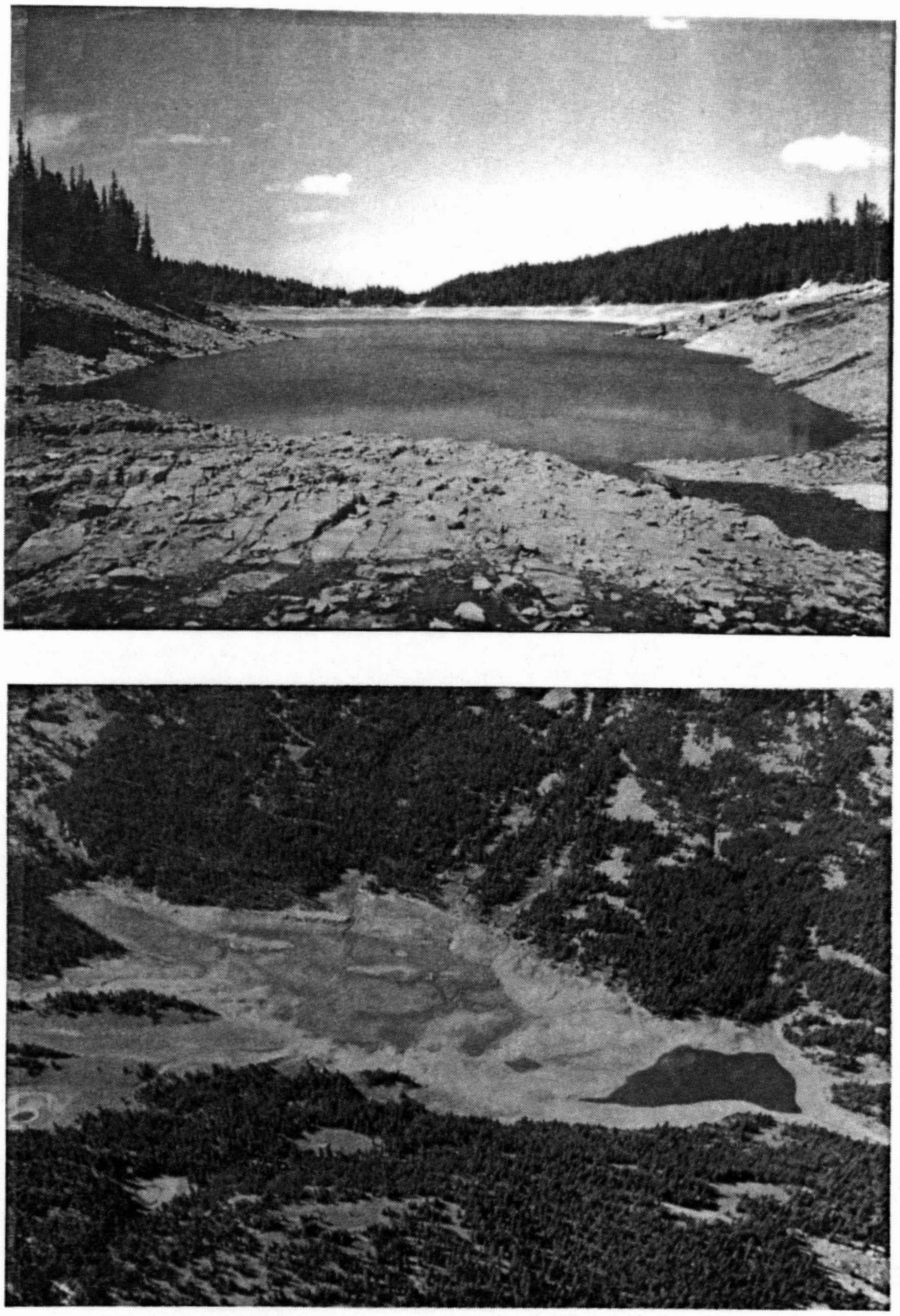

Figure 42. June 8, 1988 (top) and October 10, 1988 (bottom) photographs showing the drainage of water through the floor of The Six Lakes during the summer, Gros Ventre Range, Wyoming. Top photograph was taken from left side of lake in bottom photograph.

Permeability in the Tensleep Sandstone is small compared to that of epikarst in the Gros Ventre ground water system. Consequently, the water table of the Tensleep aquifer slopes from the recharge areas on the backlimb to springs at the lowest Tensleep outcrop.

Many perennial 0.25 to 1 ft^3/sec springs discharge from the Tensleep aquifer (Figure 6). Such discharges are much smaller than many of the ephemeral epikarst springs in the Gros Ventre ground water system. However, because of their abundance and small seasonal recessions, springs from the Tensleep aquifer are the major source of water for fall and winter stream flows on the backlimb of the eastern Gros Ventre Range within the study area.

The largest spring discharging from the Tensleep aquifer is Kendall warm spring which issues from fractured Phosphoria Formation along the crest of Warm Spring anticline adjacent to the Green River (figure 6). The constant 7 ft^3/sec discharge and the 1000 mg/l total dissolved solids concentration of the water indicates long flow paths to this spring. This flow is probably from the north and south through extensional fractures along the crest of the anticline.

CHAPTER VII

LATE PLIOCENE AND PLEISTOCENE EVOLUTION OF GROUND WATER CIRCULATION IN THE FORELIMB OF THE EASTERN GROS VENTRE RANGE

The purpose of this chapter is to describe how the present groundwater circulation patterns in the forelimb of the eastern Gros Ventre Range evolved through late Pliocene and Pleistocene time. The scenario presented here is necessarily speculative because accurate timing of erosional events is unavailable. However, the scenario presented conforms to the known geomorphic history of the Gros Ventre Range and surrounding areas.

Late Tertiary and Quaternary Geomorphic History of the Gros Ventre Range

The Gros Ventre Range was nearly buried by early Tertiary sediments at the close of early Eocene time. These sediments filled the Hoback Basin to at least the 9921 foot elevation of Pass Peak as shown by Dorr and others (1977). Little is known of the period between middle Eocene and late Miocene time as no sediments of this age are preserved in the Hoback Basin. However, Dorr and others (1977) concluded that a thick cover of early Tertiary sediments persisted into Pliocene time which was probably graded to the subsummit surface of the Wind River Range.

Dorr and others (1977) demonstrate that southeast flowing streams drained the south flank of the Gros Ventre Range during late Pliocene time. These streams joined the east flowing ancestral Hoback River which was tributary to the Green River as shown on Figure 43. Similarly, on the north flank of the Gros Ventre Range, Love (personal communication) and Hansen (1985) demonstrate that the ancestral Gros Ventre River flowed southeastward through what is now the Kinky Creek valley and entered the upper Green River system as shown on Figure 43.

Exhumation of the Gros Ventre Range began when Plio-Pleistocene regional uplift in northwest Wyoming resulted in steeper gradients in the ancestral Green River system. Responding to the increased gradients, the ancestral Hoback River removed at least 2000 feet of early Tertiary sediment from the Hoback Basin. The Rim, shown on Figure 43, is the western edge of what remains today of this southeast sloping early Pleistocene drainage surface (Dorr and others, 1977). It forms the modern divide between the Hoback and Green River drainages. The present 8000 foot elevation of The Rim reveals that in early Pleistocene time the Hoback Basin was still filled above the 8000 foot level.

Beginning in middle Pleistocene time, increased gradients in the Snake River system caused headward erosion

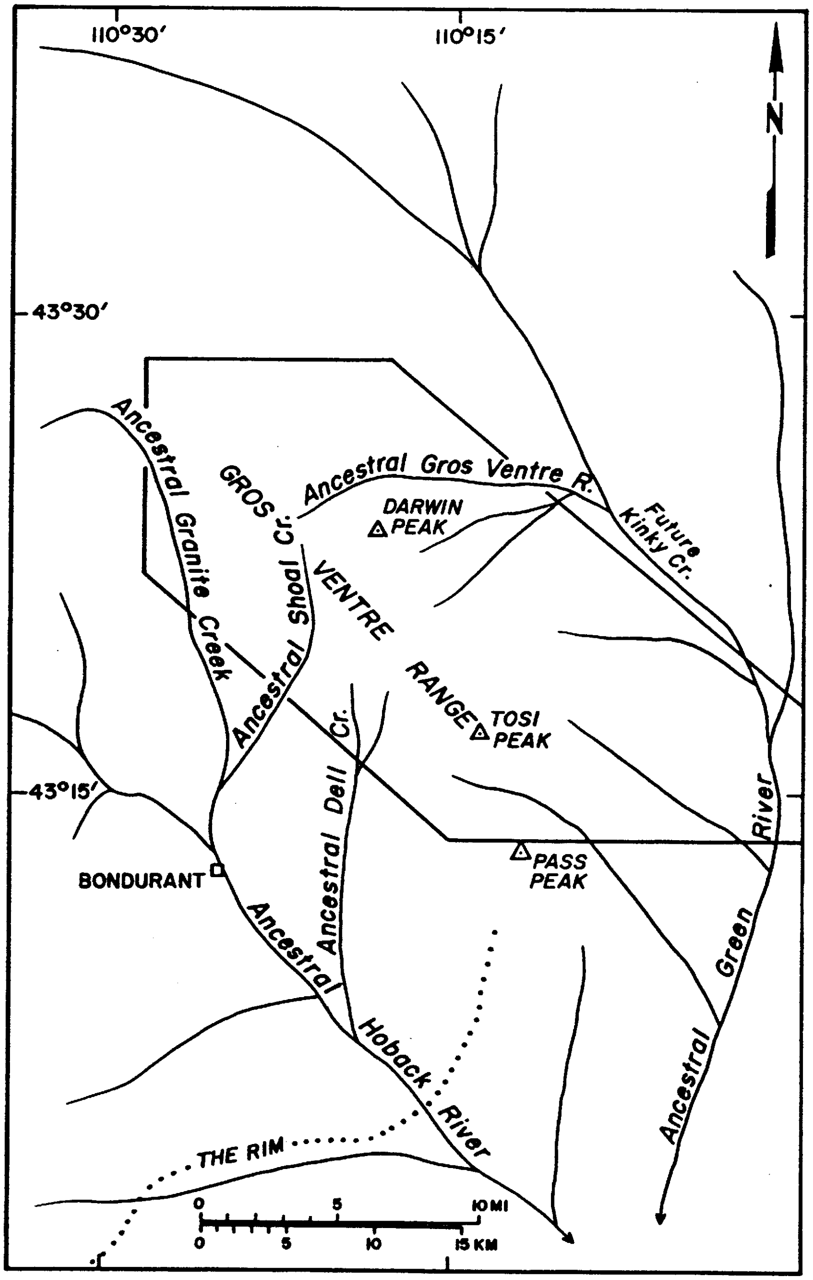

Figure 43. Map showing the reconstructed early Pleistocene surface drainage pattern around the Gros Ventre Range, Wyoming. The entire area was drained by the ancestral Green River. Map shows the present location of The Rim which is the western edge of what remains today of the southeast sloping early Pleistocene drainage surface. Modified from Dorr et al (1977) and Lackey (1974).

of west flowing rivers on both the north and south flanks of the Gros Ventre Range. The Hoback River, responding to the steeper gradients of the Snake River, increased its drainage area to the east into the Hoback Basin south of the study area (Dorr and others, 1977). The Hoback river captured Granite, Shoal, Dell, and Jack creeks on the south flank of the study area as shown on Figure 44. Similarly, the Gros Ventre River cut headward to the east on the north flank of the Gros Ventre Range and captured the upper Gros Ventre River near its present confluence with Kinky Creek. See Figure 44.

The streams draining the Gros Ventre Range then cut deeply into their beds. Modern Granite Creek flows at an elevation of 7000 feet where it crosses the Cache Creek thrust revealing at least 1000 feet of incision below the level of The Rim. Likewise, the modern Gros Ventre River is incised 650 feet below the level of its former east-flowing route through the Kinky Creek valley.

Response of Ground Water Circulation to Late Tertiary and Quaternary Geomorphic Events

Groundwater circulation patterns in a mountain range are controlled by the elevation of downgradient springs. Spring elevations in the Gros Ventre Range are localized by the structural geometry of the aquifers and the erosional history of the range. Consequently, ground water

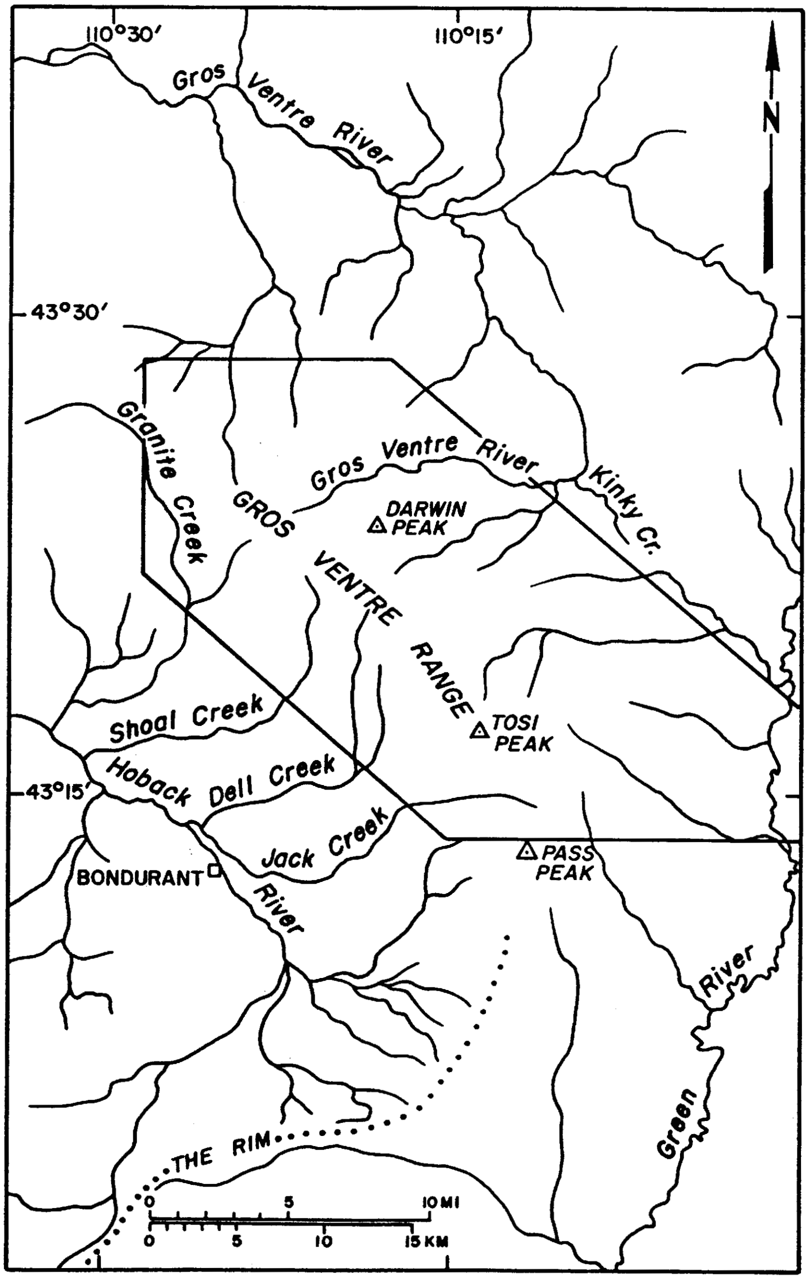

Figure 44. Map showing the modern surface drainage pattern around the Gros Ventre Range, Wyoming. The Rim is the modern divide between the Hoback and Green River drainages.

circulation does not necessarily mimic surface drainage and ground water systems need not be captured simultaneously with surface drainage systems.

The overall structural geometry of the Paleozoic rocks in the Gros Ventre Range was established by the end of extensional faulting in early Pliocene time. Subsequently, the spring elevations of forelimb Paleozoic rocks have adjusted to: (1) early Pleistocene stripping of sediments from the Hoback basin by the southeast flowing ancestral Hoback River drainage, (2) middle and late Pleistocene drainage capture and incision by the west flowing Hoback River, and (3) late Pleistocene glacial scouring of the Granite, Shoal, and Dell creek drainages.

Drainage from the south flank of the Gros Ventre Range was southeastward into the Green River prior to middle Pleistocene time. As a result, the Paleozoic rocks along the New Fork fault near The Elbow were the lowest discharge points for ground water in the Shoal Creek-New Fork fault zone. Ground water circulating in the Paleozoic rocks in the western half of the study area flowed eastward along the Shoal Creek-New Fork fault zone to springs in this area as shown on Figure 45.

The pre-middle Pleistocene east directed ground water flow resulted in the development of large fracture and karst permeability along the Shoal Creek-New Fork fault system. Mathematical modelling by Forster and Smith (1988)

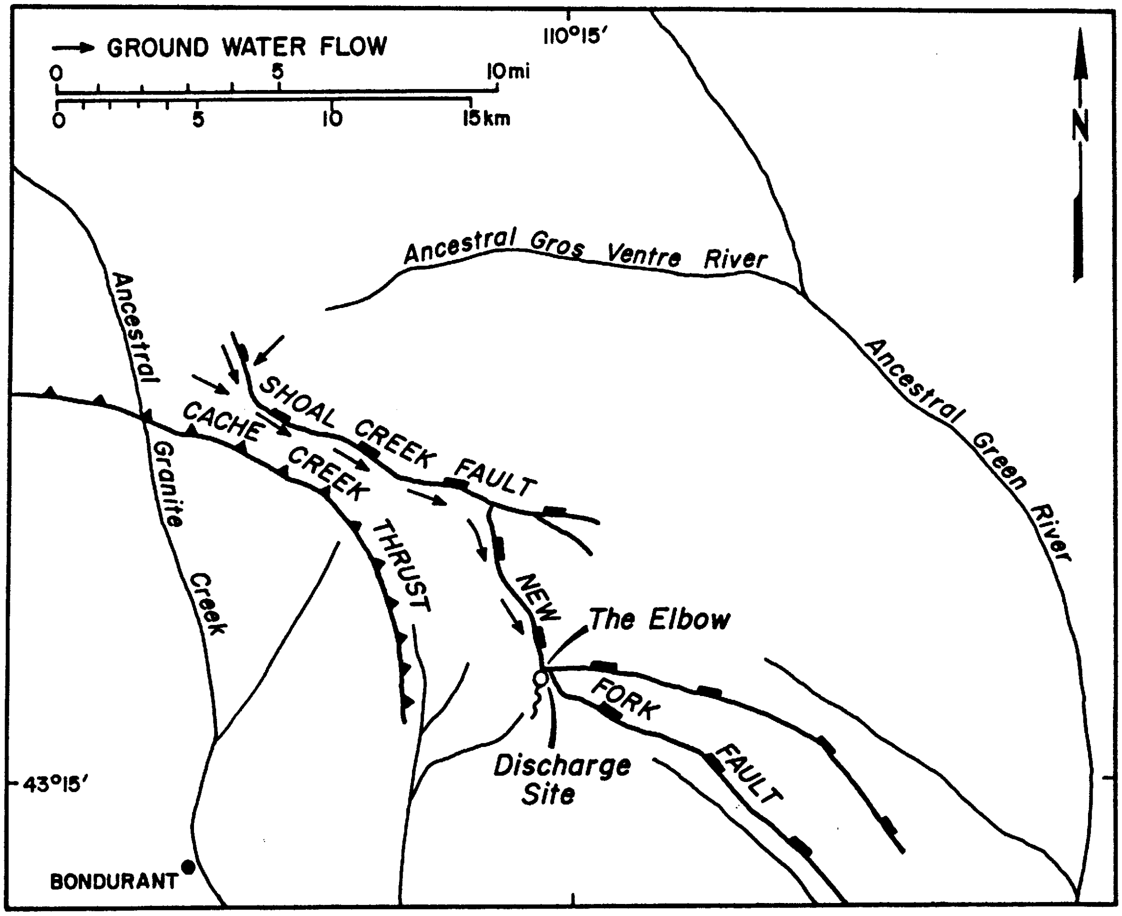

Figure 45. Map showing the reconstructed early Pleistocene ground water flow patterns along the Shoal Creek-New Fork fault system as adjusted to the early Pleistocene surface drainage system around the Gros Ventre Range, Wyoming. Ground water recharges along the faults and flows to a discharge site along the New Fork fault near The Elbow.

demonstrates that the amount of ground water in a mountain range that flows to a fault zone depends in part on fault zone permeability. If fault zone permeability increases over time through karstification and piping, as it did along the Shoal Creek-New Fork fault zone, the volume of rock drained will also increase.

As karstification proceeded through Pleistocene time the Shoal Creek-New Fork fault zone became the primary discharge route for ground water in Paleozoic rocks in the forelimb. The Shoal Creek-New Fork fault zone still transmits most of the ground water in the forelimb today. In mid-September 1988 springs from the aquifer along the fault zone discharged over 80 percent of the water in streams draining the forelimb.

The middle and late Pleistocene capture and glacial scouring of Granite, Shoal, and Dell creeks formed new outlets for ground water in the Shoal Creek-New Fork fault zone. Ground water discharge at the new outlets has redirected the ground water flow pattern in parts of the forelimb east of Granite Creek.

Late Pleistocene glacial scouring of Granite Creek exposed the Cache Creek thrust and the Death Canyon Limestone at an elevation of 7000 feet, 1000 feet below the present water table of the aquifer in the New Fork ground water system. Ground water discharge in the area of Twin springs initiated flow towards Granite Creek and caused the

Swift Creek ground water system to separate from the New Fork system.

The steep hydraulic gradient from the Shoal Creek-New Fork fault zone to Twin springs facilitated rapid karstification of the Death Canyon Limestone in the Swift Creek system. As karstification proceeded, the developing Swift Creek system captured ground water from the east flowing system in the Shoal Creek-New Fork fault zone as shown on Figure 46. This capture was confirmed by dye trace 1. However, the probable eastward loss of dye in trace 2 indicates that ground water capture from the fault zone has not progressed very far to the east.

Pleistocene incision and glacial scouring of Dell and East Dell creeks produced spring elevations of about 8150 feet at Dell and East Dell springs. Discharge from Dell and East Dell springs caused reversal of ground water flow along part of the New Fork fault. A ground water flow divide now exists along the north trending segment of the New Fork fault as shown on Figures 6 and 46.

Sediment has been stripped from the Jack Creek valley since Jack Creek was captured in late Pleistocene time. As this occurred, the New Fork fault was progressively exposed at lower elevations to the east. See the elevations along fault trace on Figure 6. As a result, the position of Jack Creek spring has migrated eastward from the former position near The Elbow to its present position shown in Figure 46.

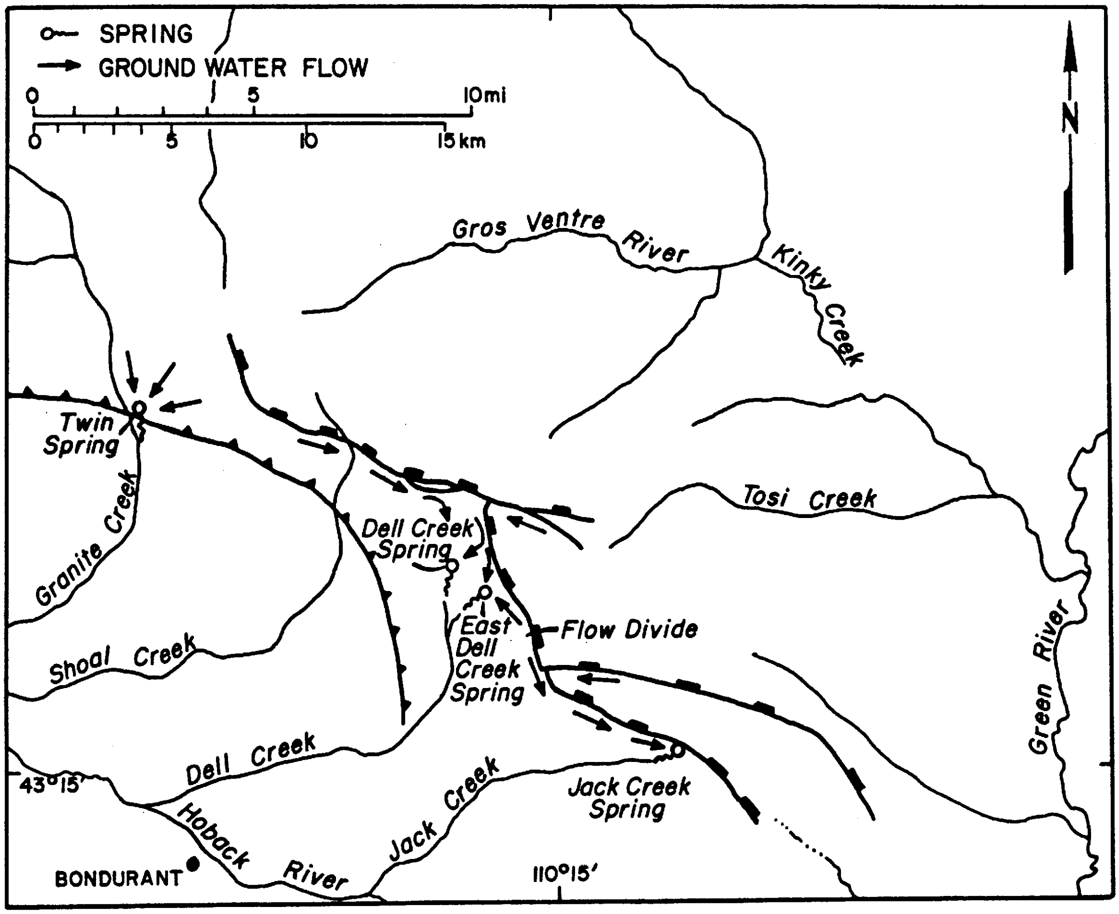

Figure 46. Map of modern ground water circulation patterns in the forelimb of the eastern Gros Ventre Range, Wyoming. Flow from the western Shoal Creek fault is now towards Twin springs. Modern discharge from the New Fork ground water system at Dell and East Dell springs reversed flow along part of the north trending segment of the New Fork fault.

CHAPTER VIII

CONCLUSIONS

1. The eastern Gros Ventre Range was uplifted and thrust west-southwest by successive displacement beginning along the Cache Creek Blind thrust, progressing to the Cache Creek thrust, and ending along the Shoal Creek-New Fork fault system during late Paleocene and early Eocene time.

2. The New Fork reverse fault is structurally linked to the Shoal Creek fault along what has previously been mapped as the North Elbow Mountain normal fault.

3. Shortening across the Shoal Creek and New Fork faults was synchronous and westward within the hanging wall of the Cache Creek thrust after middle early Eocene time. This occurred after movement along the Cache Creek thrust had ceased.

4. In the undeformed backlimb of the eastern Gros Ventre Range, the Paleozoic rocks comprise the Death Canyon, Madison, and Tensleep aquifers. The small intergranular, intercrystalline, and fracture

permeabilities in these aquifers have little influence on ground water circulation in the range.

5. Large fracture and karst permeabilities associated with fault zones and epikarst permeabilities near the surface of carbonate beds have a much larger influence on ground water circulation in the eastern Gros Ventre Range than the smaller permeabilities of the undeformed aquifers.

6. Three types of ground water storage occur in the eastern Gros Ventre Range: (1) storage in a regional aquifer, (2) water in transit in deep but unsaturated karst systems, and (3) transient storage in epikarst zones perched above regional aquifers.

7. The unsaturated Paleozoic rocks in the forelimb of the eastern Gros Ventre Range are characterized by large vertical fracture and karstic permeabilities.

8. In the New Fork ground water system in the forelimb, water infiltrating Paleozoic rocks recharges an aquifer comprised of the entire fracture integrated Paleozoic section. Discharge from this aquifer supplies most of the fall and winter stream flow from the forelimb.

9. In the Swift Creek ground water system in the forelimb, water infiltrating Paleozoic rocks flows through a deep karst system in the Death Canyon Limestone and discharges without reaching an aquifer.

10. Epikarst, which develops in outcrops of the Madison Limestone and Bighorn Dolomite on the backlimb of the eastern Gros Ventre Range, transmits the majority of snow melt in the area to ephemeral springs during the summer.

11. Transient storage in the backlimb epikarsts is depleted during the summer and provides very little water to fall and winter stream flows.

12. Diversion of snow melt through backlimb epikarsts to ephemeral springs decreases the recharge to the underlying regional aquifers.

13. The zone of saturation of the regional Madison aquifer in the backlimb is below the lowest Madison Limestone outcrop. Therefore this aquifer does not discharge on the backlimb.

14. Ground water discharged from the Tensleep aquifer supplies the majority of fall and winter stream flows on the backlimb.

15. A late Pliocene-early Pleistocene east directed groundwater circulation system along the Shoal Creek-New Fork fault zone was fragmented by stream incision and glacial scouring during middle Pleistocene to Recent time. This resulted in a reversal in the flow direction of ground water in parts of the fault zone.

APPENDICES

APPENDIX A

UNITED STATES GEOLOGICAL SURVEY WELL AND SPRING LOCATION SYSTEM

Appendix A

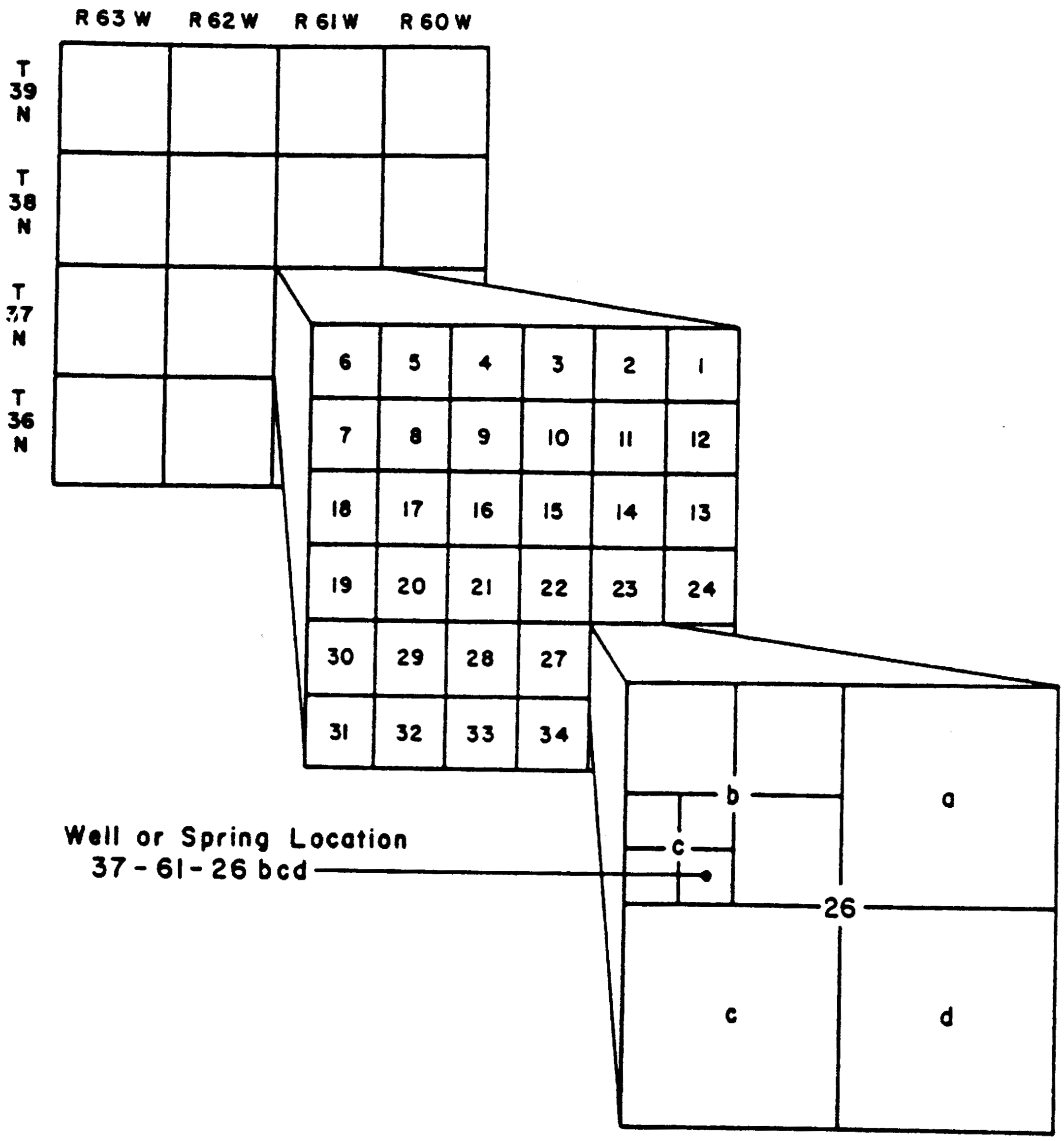
R 63 W
R 62 W
R 61 W
R 60 W
T 39 N
T 38 N
T 37 N
T 36 N
6
5
4
3
2
1
7
8
9
10
11
12
18
17
16
15
14
13
19
20
21
22
23
24
30
29
28
27
31
32
33
34
b
a
c
26
c
d
Well or Spring Location
37 - 61 - 26 bcd

APPENDIX B

INVENTORY OF SPRINGS IN THE EASTERN GROS VENTRE RANGE

Appendix B

Spring Number[a]	Location[b]	Producing Unit[c]	Discharge[d] (ft3/sec)
1	41-113-11dca	Pt	1
2	40-113-11aab	Mm	3 - 0
3	40-113-11aad	Mm	3 - 0
4	40-114-24aad	Mm	2 - 0.5
5	40-113-30bca	Cg	0.5 - 0.1
6	40-113-21add	Cgd	1
7	40-113-21daa	Cgd	1
8	40-113-13acd	Mm	5 - 0
9	40-112-30bac	Cgd	0.5 - 0
10	40-112-19dcc	Cg	0.25 - 0
11	40-112-20cac	Ob	0.25 - 0
12	40-112-20ada	Mm	1 - 0
13	40-112-21bbc	Mm	0.25 - 0
14	40-112-21abc	Mm	4 - 0
15	40-112-21aac	Mm	6 - 0
16	40-112-21aad	Mm	1 - 0
17	40-112-14dbc	Pt	0.25
18	40-112-14dca	Pt	0.25
19	40-112-14ddb	Pt	0.5
20	40-112-13ccb	Pt	0.5
21	40-112-13cdc	Pt	0.5
22	40-112-13dcb	Pt	0.5
23	40-112-13dcc	Pt	0.5

Spring Number[a]	Location[b]	Producing Unit[c]	Discharge[d] (ft3/sec)
24	40-112-13ddc	Pt	0.5
25	40-112-13ddd	Pt	0.5
26	40-111-19bca	Pt	1
27	40-113-31dbd	Cgd	0.25 - 0
28	40-113-31ddc	Cgd	4 - 0.5
29	39-113-6dac	Qt	1
30	39-113-6ddd	Cf	0.1
31	39-113-7aaa	Ql	53 - 1.6
32	39-113-8bad	Ql	0.25 - 0
33	39-113-9cbd	Qa	0.1
34	39-113-9cba	Qg	0.1
35	39-113-9acb	Qa	15 - 1.5
36	39-113-9acc	Qa	2 - 0.5
37	39-113-4ddd	Mm	0.5 - 0
38	39-113-10ada	Cgd	<0.1
39	39-113-10dbd	Qt	0.5 - 0
40	39-113-15acc	Ql	0.25
41	39-113-14cdb	Ql	0.05
42	39-113-13cdb	Mm	4 - 0
43	39-113-13cac	Mm	3 - 0
44	39-113-13dba	Mm	0.5
45	39-113-13daa	Mm	1 - 0
46	39-113-13add	Cg	8 - 0.5

Spring Number[a]	Location[b]	Producing Unit[c]	Discharge[d] (ft3/sec)
47	39-112-7ccc	pC	3 - 0.5
48	39-113-12dad	Cf	0.05 - 0
49	39-112-7cca	pC	2 - 0
50	39-112-17dcb	Mm	5 - 0
51	39-112-4dcb	Cg	0.25 - 0
52	39-112-10cab	Ob	0.5 - 0
53	39-112-3dbc	Mm	0.5 - 0
54	40-112-35dbc	Mm	0.5 - 0
55	39-112-11cdb	Mm	10 - 0
56	39-112-11aab	Mm	0.25 - 0
57	39-112-11adb	Mm	0.25 - 0
58	39-112-12bab	Mm	6 - 0
59	39-112-12bad	Mm	1 - 0
60	39-111-6abd	Pt	0.5
61	40-111-32ccb	Pp	0.1
62	39-112-28bca	Pp	15 - 0
63	39-112-28bcd	Pp	3
64	39-112-28cbd	Jgs	0.1
65	39-112-27cca	Pp	17-11
66	39-112-22adc	Pa	0.1 - 0
67	39-111-19dcc	Mm	1.5 - 0
68	39-111-19bcc	Pt	0.5
69	39-111-20bcc	Pt	0.5

Appendix B (continued)

Spring Number[a]	Location[b]	Producing Unit[c]	Discharge[d] (ft3/sec)
70	39-111-24bda	Mm	6 - 0.1
71	39-110-19bdb	Pt	0.5
72	39-110-20bba	Pt	0.25
73	39-110-20bab	Pt	0.25
74	38-111-17dcd	Pt	18 - 12
75	38-111-21bca	Pt	0.25
76	38-110-20bcc	Pt	0.25
77	38-110-19dad	Pt	0.25
78	38-110-2caa	Pp	8
79	38-110-11caa	Pp	0.5

a - spring numbers refer to springs shown on figure 6.

b - location according to U.S. Geological Survey well and spring numbering system shown in appendix A.

c - explanation of stratigraphic unit abbreviations on figure 5.

d - range of discharge rates observed during 1987-1988

APPENDIX C

MAJOR ION ANALYSES FOR GROUND WATER SAMPLES FROM PALEOZOIC ROCKS IN THE EASTERN GROS VENTRE RANGE

Appendix C

Spring Number[a]	Location[b] Date collected	Water Yielding Unit[c]	pH (lab)	Temp. (°F)	Ca++ mg/l meq/l	Mg++ mg/l meq/l	K+ mg/l meq/l	Na+ mg/l meq/l	NH4+ mg/l meq/l	Cl- mg/l meq/l	F- mg/l meq/l	PO4- mg/l meq/l	NO3- mg/l meq/l	SO4-- mg/l meq/l	HCO3-+CO3-- mg/l meq/l	Si mg/l	Charge balance error	TDS Calc. mg/l
1	41-113-11dca 6-8-88	Pc	7.58	-	53.91 2.690	20.55 1.690	0.00 0.000	0.23 0.010	0.00 0.000	1.42 0.040	0.00 0.000	0.00 0.000	0.00 0.000	68.20 1.420	181.21 2.970	3.02	0.5%	233.41
6	40-113-21add 6-30-88	Cgd	7.72	-	28.66 1.430	10.70 0.880	0.00 0.000	0.00 0.000	0.00 0.000	0.00 0.000	0.00 0.000	0.00 0.000	0.00 0.000	0.48 0.010	137.28 2.250	0.78	1.1%	107.34
9	40-112-30bac 7-22-88	Cgd	7.91	46	27.45 1.370	4.86 0.400	0.39 0.010	0.00 0.000	0.00 0.000	0.00 0.000	0.00 0.000	0.00 0.000	0.00 0.000	5.76 0.120	98.23 1.610	0.83	1.4%	86.77
13	40-112-21bbc 7-22-88	Mm	8.01	39	28.06 1.400	7.30 0.600	0.00 0.000	0.00 0.000	0.00 0.000	0.00 0.000	0.00 0.000	0.00 0.000	0.00 0.000	1.44 0.030	118.36 1.940	0.62	0.8%	94.99
25	40-112-13ddd 6-13-88	Pc	7.57	-	67.13 3.350	24.44 2.010	0.00 0.000	0.23 0.010	0.00 0.000	1.06 0.030	0.00 0.000	0.00 0.000	0.00 0.000	122.00 2.540	172.67 2.830	3.11	0.3%	299.77
28	40-113-31dbd 8-11-87	Cgd	-	41	34.47 1.720	14.47 1.190	0.35 0.009	0.44 0.019	0.00 0.000	0.39 0.011	-	0.00 0.000	0.00 0.000	3.31 0.069	187.92 3.080	1.76	3.6%	147.59
29	39-113-6dac 8-11-87	Qt	-	106	30.66 1.530	6.32 0.520	8.99 0.230	181.23 7.880	0.00 0.000	138.30 3.900	-	0.00 0.000	0.00 0.000	145.53 3.030	208.05 3.410	26.40	0.9%	639.74
29	39-113-6dac 4-2-88	Qt	8.32	112	30.06 1.500	5.51 0.453	12.04 0.308	203.08 8.830	0.00 0.000	150.71 4.250	5.32 0.280	0.09 0.003	0.50 0.008	157.54 3.280	220.87 3.620	27.69	1.6%	673.45
30a	39-113-6ddd 6-2-87	Cf	-	>120	26.25 1.310	3.28 0.270	1.41 0.036	255.29 11.100	0.00 0.000	228.72 6.450	-	0.00 0.000	0.00 0.000	182.04 3.790	185.48 3.040	39.70	2.2%	827.89
30b	39-113-6ddd 4-2-88	Cf	8.27	>120	24.65 1.230	2.54 0.209	17.08 0.437	266.10 11.570	0.00 0.000	233.69 6.590	6.84 0.360	0.09 0.003	0.81 0.013	180.12 3.750	190.97 3.130	39.38	1.5%	825.82
31a	39-113-7aaa 6-2-87	Ql	-	43	25.25 1.260	7.54 0.620	0.47 0.012	3.86 0.168	0.00 0.000	3.44 0.097	-	0.00 0.000	0.00 0.000	11.29 0.235	116.53 1.910	1.98	4.2%	111.13
31b	39-113-7aaa 4-1-88	Ql	8.27	56	29.06 1.450	10.24 0.842	2.11 0.054	29.21 1.270	0.00 0.000	25.74 0.726	0.85 0.045	0.00 0.000	0.00 0.000	36.02 0.750	141.55 2.320	8.38	3.0%	202.84
31c	39-113-7aaa 4-1-88	Ql	8.26	56	29.06 1.450	10.30 0.847	1.99 0.051	28.29 1.230	0.00 0.000	24.47 0.690	0.84 0.044	0.00 0.000	0.00 0.000	35.06 0.730	140.33 2.300	5.42	2.5%	199.01
31d	39-113-7aaa 5-19-88	Ql	7.39	44	30.06 1.500	8.63 0.710	0.00 0.000	0.46 0.020	0.00 0.000	5.67 0.160	0.00 0.000	0.00 0.000	0.00 0.000	7.68 0.160	124.47 2.040	1.93	2.8%	113.71
31e	39-113-7aaa 5-27-88	Ql	7.57	42	24.05 1.200	7.05 0.580	0.00 0.000	0.23 0.010	0.00 0.000	2.48 0.070	0.00 0.000	0.00 0.000	0.00 0.000	3.84 0.080	103.72 1.700	1.26	1.6%	88.66
31f	39-113-7aaa 6-5-88	Ql	7.6	42	20.24 1.010	5.84 0.480	0.00 0.000	0.00 0.000	0.18 0.010	0.71 0.020	0.00 0.000	0.00 0.000	0.00 0.000	2.88 0.060	86.64 1.420	1.02	0.0%	72.27
31g	39-113-7aaa 7-1-88	Ql	7.89	-	20.24 1.010	5.71 0.470	0.00 0.000	0.23 0.010	0.00 0.000	3.55 0.100	0.00 0.000	0.00 0.000	0.62 0.010	8.17 0.170	79.32 1.300	1.49	2.9%	77.52
31h	39-113-7aaa 7-16-88	Ql	7.87	44	22.65 1.130	7.30 0.600	0.78 0.020	5.29 0.230	0.54 0.030	3.19 0.090	0.00 0.000	0.32 0.010	0.00 0.000	11.53 0.240	90.30 1.480	1.81	4.2%	95.45
31i	39-113-7aaa 8-22-88	Ql	8.02	-	25.65 1.280	8.51 0.700	0.78 0.020	11.73 0.510	0.00 0.000	6.74 0.190	0.00 0.000	0.00 0.000	0.00 0.000	17.29 0.360	104.94 1.720	2.59	5.0%	122.30
32	39-113-8bad 5-19-88	Ql	7.19	39	36.07 1.800	12.28 1.010	0.00 0.000	0.46 0.020	0.00 0.000	0.71 0.020	0.00 0.000	0.00 0.000	0.00 0.000	5.76 0.120	169.62 2.780	1.29	1.6%	138.69
33	39-113-9cbd 6-2-87	Qa	-	39	58.92 2.940	10.82 0.890	0.59 0.015	2.02 0.088	0.00 0.000	0.57 0.016	-	0.00 0.000	0.00 0.000	2.02 0.042	258.69 4.240	2.60	4.4%	204.73

Spring Number[a]	Location[b] Date collected	Water Yielding Unit[c]	pH (lab)	Temp. (°F)	Ca++ mg/l meq/l	Mg++ mg/l meq/l	K+ mg/l meq/l	Na+ mg/l meq/l	NH4+ mg/l meq/l	Cl- mg/l meq/l	F- mg/l meq/l	PO4- mg/l meq/l	NO3- mg/l meq/l	SO4-- mg/l meq/l	HCO3-+CO3-- mg/l meq/l	Si mg/l	Charge balance error	TDS Calc. mg/l
34	39-113-9cba 6-2-87	Qg	-	42	58.12 2.900	17.39 1.430	0.43 0.011	1.20 0.052	0.00 0.000	0.60 0.017	-	0.00 0.000	0.00 0.000	1.63 0.034	288.59 4.730	3.19	4.2%	224.46
35a	39-113-9acb 6-3-87	Qa	-	39	41.08 2.050	11.43 0.940	0.27 0.007	0.51 0.022	0.00 0.000	0.35 0.010	-	0.00 0.000	0.00 0.000	3.17 0.066	195.24 3.200	1.60	4.1%	154.42
35b	39-113-9acb 4-1-88	Qa	8.33	39	31.46 1.570	10.58 0.870	0.23 0.006	0.46 0.020	0.00 0.000	0.39 0.011	0.00 0.000	0.00 0.000	0.50 0.008	7.68 0.160	154.36 2.530	1.67	4.7%	127.21
36	39-113-9acc 4-1-88	Qa	8.21	40	72.34 3.610	18.63 1.532	0.55 0.014	0.69 0.030	0.18 0.010	5.67 0.160	0.00 0.000	0.00 0.000	0.00 0.000	14.89 0.310	331.30 5.430	4.12	6.3%	275.67
37	39-113-4ddd 5-20-88	Mm	7.55	37	27.86 1.390	8.88 0.730	0.00 0.000	0.00 0.000	0.00 0.000	0.35 0.010	0.00 0.000	0.00 0.000	0.00 0.000	4.32 0.090	120.20 1.970	1.40	1.2%	100.51
38	39-113-10ada 6-7-87	pC	-	43	8.22 0.410	0.73 0.060	0.39 0.010	1.15 0.050	0.00 0.000	0.35 0.010	-	0.00 0.000	0.00 0.000	6.82 0.142	25.02 0.410	2.84	2.9%	32.80
39	39-113-10dbd 6-20-87	Qt	-	34	20.24 1.010	5.59 0.460	0.59 0.015	0.85 0.037	0.00 0.000	0.18 0.005	-	0.00 0.000	0.00 0.000	7.25 0.151	90.30 1.480	0.71	3.6%	79.81
40	39-113-15acc 6-21-87	Th	-	40	66.33 3.310	10.58 0.870	0.39 0.010	1.26 0.055	0.00 0.000	0.21 0.006	-	0.00 0.000	0.00 0.000	30.55 0.636	237.95 3.900	1.55	3.4%	227.88
41	39-113-14cca 6-20-87	Ql	-	44	53.31 2.660	7.30 0.600	0.27 0.007	1.31 0.057	0.00 0.000	0.14 0.004	-	0.00 0.000	0.00 0.000	16.57 0.345	198.90 3.260	1.80	4.1%	178.58
42	39-113-13cdb 6-20-87	Mm	-	38	26.65 1.330	5.71 0.470	0.20 0.005	0.18 0.008	0.00 0.000	0.25 0.007	-	0.00 0.000	0.00 0.000	5.91 0.123	111.04 1.820	1.14	3.6%	94.64
43	39-113-13cac 6-18-87	Mm	-	40	27.05 1.350	6.93 0.570	0.31 0.008	0.39 0.017	0.00 0.000	0.28 0.008	-	0.00 0.000	0.00 0.000	9.13 0.190	114.70 1.880	1.57	3.3%	102.07
45	39-113-13daa 6-21-87	Mm	-	38	26.25 1.310	7.42 0.610	0.43 0.011	0.76 0.033	0.00 0.000	0.18 0.005	-	0.00 0.000	0.00 0.000	12.97 0.270	113.48 1.860	2.32	4.2%	106.12
46	39-113-13add 6-21-87	Cg	-	36	20.64 1.030	5.35 0.440	0.23 0.006	0.25 0.011	0.00 0.000	0.11 0.003	-	0.00 0.000	0.00 0.000	3.55 0.074	92.74 1.520	0.05	3.6%	75.79
47	39-112-7ccc 6-21-87	pC	-	40	18.64 0.930	2.31 0.190	0.86 0.022	0.80 0.035	0.00 0.000	0.21 0.006	-	0.00 0.000	0.00 0.000	9.61 0.200	63.45 1.040	2.05	2.8%	65.68
48	39-113-dad 6-23-87	Cf	-	43	38.28 1.910	8.51 0.700	0.47 0.012	0.48 0.021	0.00 0.000	0.46 0.013	-	0.00 0.000	0.00 0.000	2.59 0.054	169.01 2.770	2.64	3.5%	136.53
49	39-112-cca 6-23-87	pC	-	44	17.43 0.870	2.68 0.220	0.98 0.025	1.17 0.051	0.00 0.000	0.21 0.006	-	0.00 0.000	0.00 0.000	15.80 0.329	54.30 0.890	2.69	2.5%	67.67
50	39-112-dcd 7-12-87	Mm	-	38	9.22 0.460	1.22 0.100	0.16 0.004	0.28 0.012	0.00 0.000	0.07 0.002	-	0.00 0.000	0.00 0.000	2.11 0.044	35.39 0.580	1.03	4.2%	31.48
52	39-112-10cab 7-24-88	Ob	7.95	36	11.82 0.590	2.43 0.200	0.00 0.000	0.00 0.000	0.00 0.000	0.00 0.000	0.00 0.000	0.00 0.000	0.00 0.000	0.00 0.000	46.37 0.760	0.28	1.9%	37.06
58	39-112-12bab 6-14-88	Mm	7.79	-	26.65 1.330	5.11 0.420	0.00 0.000	0.00 0.000	0.00 0.000	0.00 0.000	0.00 0.000	0.00 0.000	0.00 0.000	0.00 0.000	103.72 1.700	0.60	1.4%	82.76
61	40-111-32cc 6-14-88	Pp	7.77	-	27.66 1.380	7.42 0.610	0.00 0.000	0.00 0.000	0.00 0.000	0.00 0.000	0.00 0.000	0.00 0.000	0.00 0.000	3.36 0.070	115.92 1.900	0.88	0.5%	95.43
62a	39-112-28bca 7-12-87	Pp	-	38	19.64 0.980	7.90 0.650	0.43 0.011	0.28 0.012	0.00 0.000	0.39 0.011	-	0.00 0.000	0.00 0.000	21.61 0.450	85.42 1.400	0.82	5.9%	93.07

Spring Number[a]	Location[b] Date collected	Water Yielding Unit[c]	pH (lab)	Temp. (°F)	Ca++ mg/l meq/l	Mg++ mg/l meq/l	K+ mg/l meq/l	Na+ mg/l meq/l	NH4+ mg/l meq/l	Cl- mg/l meq/l	F- mg/l meq/l	PO4- mg/l meq/l	NO3- mg/l meq/l	SO4-- mg/l meq/l	HCO3-+CO3-- mg/l meq/l	Si mg/l	Charge balance error	TDS Calc. mg/l
62b	39-112-28bca	Pp	8.01	-	43.49	12.16	0.00	0.69	0.00	0.00	0.00	0.00	0.62	42.27	132.40	1.37	2.2%	164.32
	8-18-88				2.170	1.000	0.000	0.030	0.000	0.000	0.000	0.000	0.010	0.880	2.170			
64	39-112-28cbd	Jgs	-	42	400.80	98.49	2.74	106.49	0.00	21.28	-	0.00	0.00	1556.20	-6.71	7.60	0.1%	2190.29
	7-9-87				20.000	8.100	0.070	4.630	0.000	0.600		0.000	0.000	32.400	-0.110			
65	39-112-27cca	Pp	7.78	44	31.06	9.73	0.00	1.84	0.00	1.06	0.00	0.00	0.00	24.98	102.50	1.69	4.3%	119.07
	8-18-88				1.550	0.800	0.000	0.080	0.000	0.030	0.000	0.000	0.000	0.520	1.680			
66	39-112-22adc	Pa	-	34	16.63	3.16	0.08	0.00	0.00	0.11	-	0.00	0.00	2.07	68.94	0.37	3.7%	56.31
	7-15-87				0.830	0.260	0.002	0.000	0.000	0.003		0.000	0.000	0.043	1.130			
67	39-111-19dcc	Mm	-	42	35.47	3.53	0.20	0.14	0.00	0.18	-	0.00	0.00	2.02	133.62	0.08	3.9%	107.30
	7-16-87				1.770	0.290	0.005	0.006	0.000	0.005		0.000	0.000	0.042	2.190			
70	39-111-24bda	Mm	7.4	36	40.48	10.21	0.00	0.00	0.00	1.42	0.00	0.00	0.00	9.61	158.02	1.66	0.5%	139.42
	5-22-88				2.020	0.840	0.000	0.000	0.000	0.040	0.000	0.000	0.000	0.200	2.590			
74	38-111-17dcd	Pt	7.82	42	75.95	17.02	0.00	1.15	0.00	0.35	0.00	0.00	0.00	139.77	131.79	1.55	1.6%	299.05
	8-10-88				3.790	1.400	0.000	0.050	0.000	0.010	0.000	0.000	0.000	2.910	2.160			
75	38-111-21bca	Pt	7.99	39	71.34	25.54	0.00	2.07	0.00	0.35	0.00	0.00	0.00	99.90	211.10	1.69	1.8%	303.01
	8-10-88				3.560	2.100	0.000	0.090	0.000	0.010	0.000	0.000	0.000	2.080	3.460			
77	38-110-19dad	Pt	8.16	42	39.68	17.02	0.00	0.46	0.00	0.00	0.00	0.00	0.00	14.41	184.26	1.68	1.2%	162.17
	7-20-88				1.980	1.400	0.000	0.020	0.000	0.000	0.000	0.000	0.000	0.300	3.020			
78	38-110-2cca	Pp	-	84	194.39	40.13	2.74	1.61	0.00	1.77	-	0.00	0.00	629.20	127.52	10.00	7.4%	942.54
	6-27-87				9.700	3.300	0.070	0.070	0.000	0.050		0.000	0.000	13.100	2.090			
79	38-110-11caa	Pp	-	50	234.47	79.04	7.82	13.11	0.00	8.51	-	0.00	0.00	826.13	150.70	18.97	2.4%	1262.14
	6-27-87				11.700	6.500	0.200	0.570	0.000	0.240		0.000	0.000	17.200	2.470			

a - spring numbers refer to springs shown on figure 6.

b - location according to U.S. Geological Survey well and spring numbering system shown in appendix A.

c - explanation of stratigraphic unit abbreviations on figure 5.

REFERENCES CITED

Blackstone, D.L., 1988, Precambrian basement map of Wyoming: outcrop and structural configuration: The Geological Survey of Wyoming, Map Series 27.

Blackwelder, E., 1918, New geological formations in western Wyoming: Washington Academy of Science Journal, v. 8, p 417-426.

Chapman, W., 1972, Glacial history of the northern part of the Hoback River basin west-central Wyoming (Ph.D. dissertation): Univ. Michigan, Ann Arbor, Michigan, 68 p.

Cutler, E.R., 1984, Geology of the upper Green River area, between the Gros Ventre and Wind River Mountains, Sublette County, Wyoming: (M.S. thesis): University of Wyoming, Laramie, Wyoming, 103 p.

Davidson, W.R., 1987, Petrology and environmental interpretation of the synorogenic Bacon Ridge Formation, northwest Wyoming: Wyoming Geological Association, 38th. Annual Field Conference Guidebook, p. 207-216.

Doelger, N.D., 1987, The stratigraphy of the Nugget Sandstone: Wyoming Geological Association, 38th. Annual Field Conference Guidebook, p. 163-178.

Dorr, J. A., Spearing, D. R., and Steidtmann, J. R. 1977, Deformation and deposition between a foreland uplift and an impinging thrust belt: Hoback Basin, Wyoming, Geological Society of America Special Paper 177, 82 p.

Forster, C. and Smith, L., 1988, Groundwater flow systems in mountainous terrain 2. Controlling factors: Water Resources Research, v. 24, no. 7, p. 1011-1023.

Hansen, W.R., 1985, Drainage development of the Green River Basin in southwestern Wyoming and its bearing on fish biogeography, neotectonics, and paleoclimates: The Mountain Geologist, v. 22, p. 192-204.

Hill, C., Sutherland, W., and Tierney, L., 1976, Caves of Wyoming: Geological Survey of Wyoming Bulletin 59, 230 p.

Hunter, R. B. 1987, Timing and structural relations between the Gros Ventre foreland uplift, the Prospect Thrust system, and the Granite Creek thrust system, Hoback Basin, Wyoming: Wyoming Geological Association, 38th. Annual Field Conference Guidebook, p. 109-131.

Keefer, W. R., 1963, Karst topography in the Gros Ventre mountains, northwestern Wyoming: U.S. Geological Survey Professional Paper 475-B, p. 129-130.

Keefer, W. R., 1964, Preliminary report on the structure of the southeast Gros Ventre Mountains, Wyoming. U.S. Geological Survey Professional Paper 501-D, p. 22-27.

Lackey, L. E., 1974, Late Cenozoic history of the northern and eastern Hoback Basin, Wyoming (Ph.D. dissertation): University of Michigan, Ann Arbor, Michigan, 42 p.

Lageson, D.R. 1987, Laramide uplift of the Gros Ventre range and implications for the origin of the Teton Fault, Wyoming: Wyoming Geological Association, 38th. Annual Field Conference Guidebook, p. 79-89.

Love, C.M., 1968, The geology surrounding the headwaters of Nowlin, Flat, and Granite Creeks, Gros Ventre range, Teton county, Wyoming (Master thesis): Montana State University, Bozeman, Montana, 106 p.

Love, J.D., 1973, Harebell Formation (Upper Cretaceous) and Pinyon Conglomerate (Uppermost Cretaceous and Paleocene), Northwestern Wyoming: U.S. Geological Survey Professional Paper 734-A, 54 p.

Love, J.D. 1977, Summary of Upper Cretaceous and Cenozoic stratigraphy, and of tectonics and glacial events in Jackson Hole, northwestern Wyoming: Joint Wyoming-Montana-Utah Geological Association, 29th Annual Field Conference, Guidebook, p. 585-593.

Martner, B.E., 1986, Wyoming Climate Atlas: Lincoln, London, University of Nebraska Press.

Nelson, V.E., and Church, V., 1943, Critical structures in the Gros Ventre and northern Hoback ranges, Wyoming: The Journal of Geology, v. 51, no. 3, p. 143-166.

Olson, T.J., and Schmitt, J.G., 1987, Sedimentary evolution of the Miocene-Pliocene Camp Davis Basin, Northwestern Wyoming: Wyoming Geological Association, 38th Annual Field Conference Guidebook, p. 225-243.

Sando, W.J., 1975. Stratigraphic sections of the Madison Limestone and Amsden Formation, west flank of the Bighorn Basin, Wyoming: Wyoming Geological Association, 27th Annual Field Conference, Guidebook, p. 129-137.

Sando. W.J., 1988, Madison Limestone (Mississippian) paleokarst: a geologic synthesis: in James, N.P., and Choquette, P.W., ed., Paleokarst: New York, Springer-Verlag, p. 256-277.

Sheldon, R.P., 1963, Physical Stratigraphy and mineral resources of Permian rocks in western Wyoming: U. S. Geological Survey Professional Paper 313-B, 269 p.

Simons, F.S., Love, J.D., Keefer, W.R., Harwood, D.S., and Bieniewski, C.L., 1988. Mineral resources of the Gros Ventre Wilderness study area, Teton and Sublette Counties, Wyoming: U. S. Geological Survey Bulletin 1591, 4 plates, 94 p.

Skinner, R.E., 1960. Tectonic elements of the norther Green River area of Wyoming: Wyoming Geological Association 15th Annual Field Conference Guidebook, p. 86-89.

Steidtmann, J.R., 1971, Origin of the Pass Peak Formation and equivalent early Eocene strata, central western Wyoming: Geological Society of America Bulletin, v. 82, p. 156-176.

Wanless, H.R., Belknap, R.L., and Foster, H., 1955, Paleozoic and Mesozoic rocks of Gros Ventre, Teton, Hoback, and Snake River ranges, Wyoming: Geological Society of America Memoir 63, 90 p.

Werner, E., 1974. Karst of western Wyoming - an alpine karst in Tosi Creek Basin, Gros Ventre Mountains: Contributions to Geology, v. 13, no. 1, p.41-46.